HWJS

HARVARD-WESTLAKE JOURNAL OF SCIENCE • ISSUE 4 • 2010

Cosmic rays and cloud chambers

Maximizing solar cell power

The mystery of cooling water

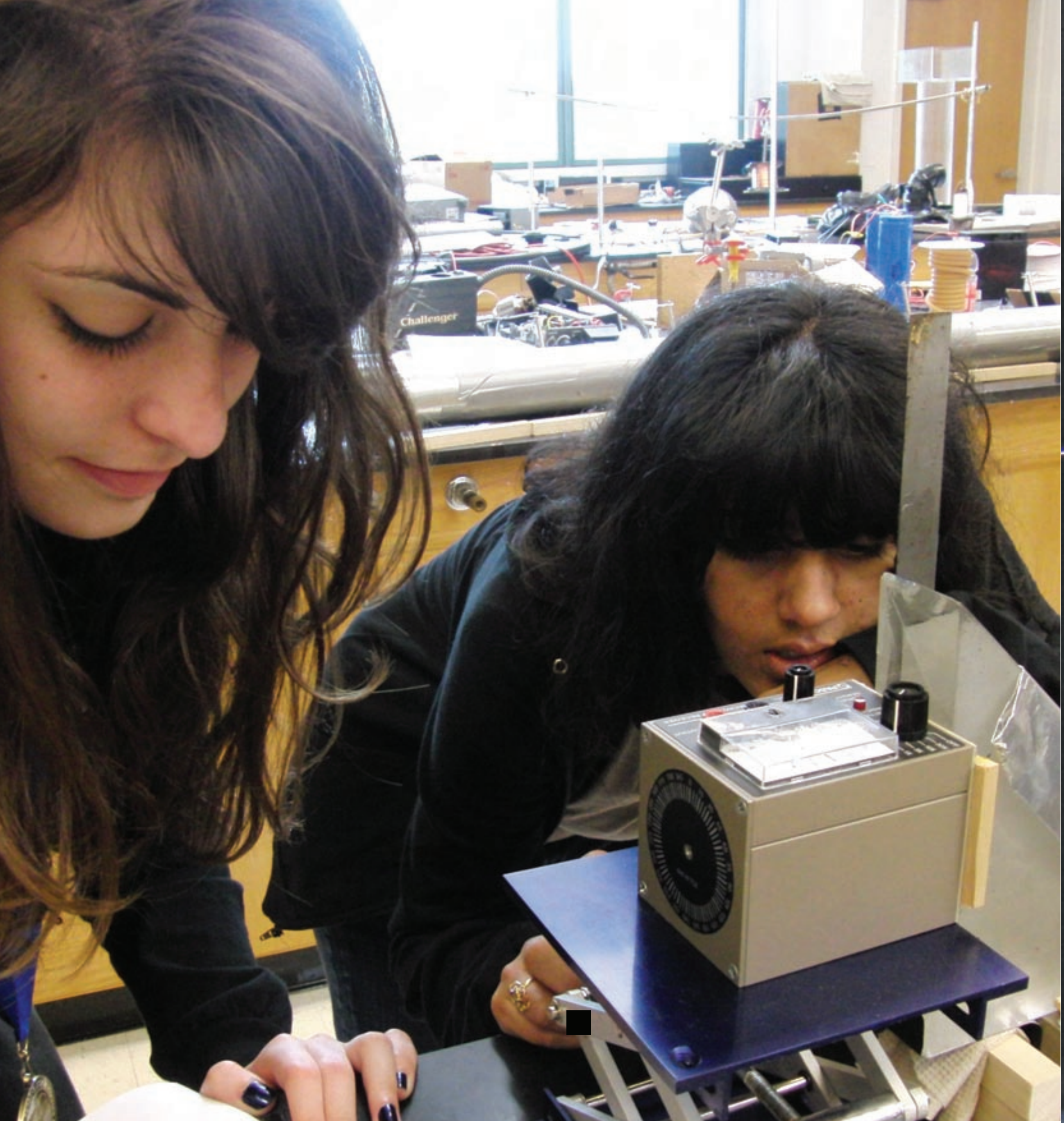

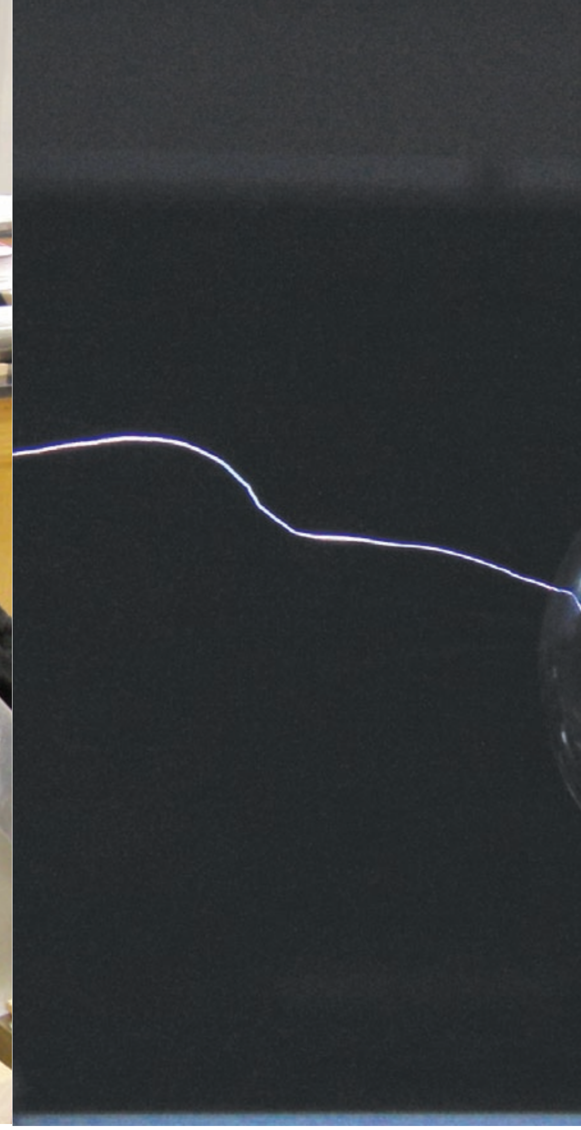

» » Harvard-Westlake

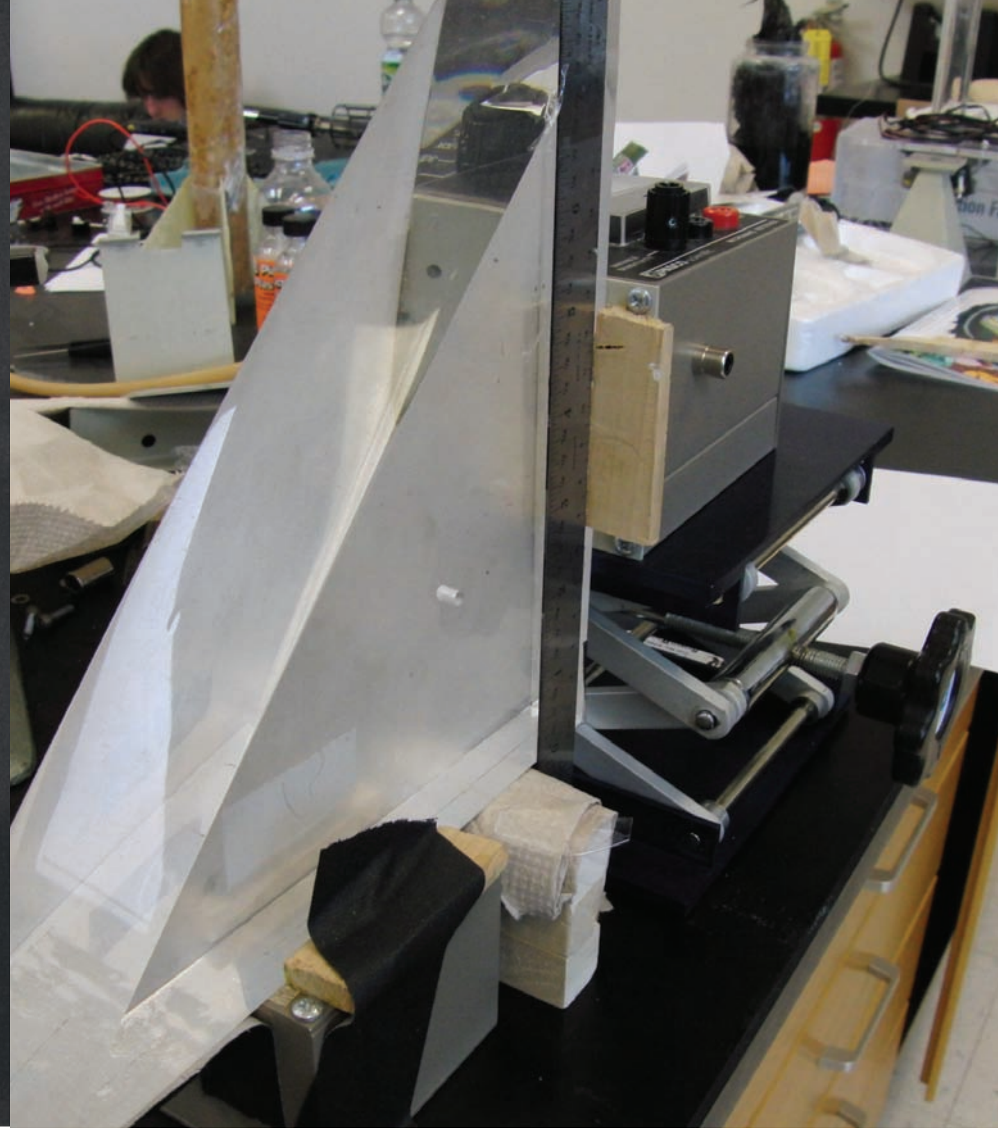

Journal of Science 2010

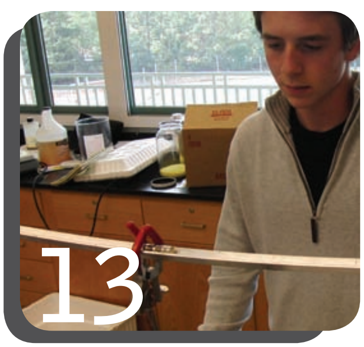

Staff

Editors in Chief: Sam Adams, Ian Cinnamon, Richard Liu

Managing Editors: Ingrid Chang, Mary Rose Fissinger, Emily Khaykin, Matt Lee, Jean Park, Alice Phillips, Daniel Rothberg

Researchers: Rohun Bansal, John Billingsley, Monica Chen, Ian Cinnamon, Jared Drooks, Charlie Fogarty, Justin Genter, Caroline Groth, Riley Guerin, Matthew Krisiloff, Kristen London, Daniel Lundberg, Riley Mate, Irene Manousiouthakis, Ilica Mahajan, Adam Moelis, Ryder Moody, Niko Natsis, Ryan Pleuger, Max Simchowitz, Andrew Wang, Jacob Witten

Advisers: Antonio Nassar, Kathleen Neumeyer

Saving the world through science

The number of scientific problems in the world we are currently confronting (global warming, Earth's weakening magnetic field, energy, diseases, etc.) seems to grow relentlessly, so we must develop clever ways to use our educational resources to generate more ideas to resolve these problems. Our educational infrastructure needs to move towards a more open, integrated, flexible and holistic system. Boosting enrollment in science programs solves only half of the problem. The other half is ensuring that skillful innovators emerge from the halls of academia, especially in high school where a quantum educational transition occurs in the lives of all young students. There we must have in place the right educational infrastructure to generate creativity, exploration and innovation along Einstein's famous quote "Imagination is more important than knowledge"; that is, the necessity for a less structured component of education.

Not only do our young scholars need time for curiosity, but they need primetime for curiosity. Students ought to find time in their busy, daily schedule for curiosity during their regular school hours. Our Harvard-Westlake Studies in Scientific Research (SSR) class provides young students during their primetime schedule with a less structured environment to inspire students to think in new, more creative ways. In order to develop more science and engineering talent to foster home-grown innovation and ensure the competitiveness of U.S. technology-based businesses we need to fire up, empower, and invest in a greater number of young minds by enabling them to start researching at an early age. This nation needs to build a comprehensive, young-age student research program without delay to motivate young minds towards solving current world scientific challenges by facilitating interactions in research among all educational levels.

Our youngsters may not have a lot of knowledge about their project at first, but they do possess significant imagination and are not yet afraid of making mistakes. SSR is a course for young science students to undertake small-scale, year-long research projects. Students discuss and collaborate with one another in their research, working through difficulties together, learning from one another, and broadening their scientific background. In SSR, the students' creativity has allowed them to explore and put into action ideas in a relaxed and playful atmosphere that is still quite constructive.

SSR students are encouraged to be daring, positive, optimistic and unrelenting and most importantly, to dream hard, which is the most inspiring element in the American character.

—Dr. Antonio Nassar
SSR Adviser

Letter from the editors

The year 2010 launches us closer into the world of tomorrow: practical electric vehicles, affordable space tourism, and legions of more practical, "green" solutions to our biggest environmental problems. Numerous start-ups and entrepreneurial projects have arisen with the bloom, such as Twitter, Aardvark, and Boxee (many of which are, evidently, IT companies). And there's still much more to come.

What Studies in Scientific Research (SSR) strives to accomplish is to bring the world of innovative engineering into the grasps of young minds. Students meet daily in a collaborative environment to share ideas, discuss projects, or simply debate on the latest scientific controversies. This journal, following the three year tradition, collects a year's worth of experimenting, discovering, debating, and healthy questioning - into a brief 24 pages.

This year's class has been one of the biggest ever, with the school hosting two sections of SSR with fifteen students each. As such, the projects have also been the most broad-ranging: from vortex ring collisions and quantum tunneling to building a more efficient go-kart. Many of the projects were inspired by current happenings in the scientific community, and others were simply started from a strong interest for the field. Nonetheless, each project is as captivating as it is unique.

As editors, we've shared great memories taking part in SSR, learning about the projects, and putting together this journal. Our task is to share with you this snippet of our year, and we sincerely hope that you enjoy what you see. Whether it be from the graphs or diagrams, the content in the papers, or the projects themselves, engage yourself in the projects, learn about something interesting. SSR's goal is to promote scientific enthusiasm within students, and HWJS's goal is to share the enthusiasm with you. So sit back, relax, and enjoy a world of curiosity and wonder.

— Sam Adams, Ian Cinnamon, Richard Liu
Editors in Chief

Brendan Kutler
1992-2009

In December 2009, friends and family were devastated to hear that Brendan Kutler had suddenly died in his sleep. He was enormously admired among his peers, teachers, and friends, and his passing left an indelible mark on all of us.

During the summer between 10th and 11th grade Brendan worked at a lab at UCLA called the Center for Embedded Networked Sensing. From the first day, everyone realized how intelligent, curious, creative, and most importantly, selfless, Brendan was. Whenever anyone had a question, whether it was about programming, image analysis, or something totally random and out of the blue, like his opinion on the best ice cream flavor at Diddy Riese, he would drop whatever he was doing, no matter how important it was, and help. Even if something at the lab wasn't working as planned... like, for example, when he spent two weeks creating a brilliant database system for storing and querying images, only to later find out he had to use a different system, Brendan wasn't upset or sad. He was a bit annoyed that his system wouldn't be used, but he took that news in stride. He was able to see the big picture and recognize that even though a specific part of his project didn't proceed as planned, overall the research he was doing was a huge success.

Brendan's passing left a permanent hole in the senior class as well as Harvard-Westlake as a whole. The scientific community has lost one of its brightest stars.

Investigating the Goos-Haenchen Shift Evanescent Waves, and Quantum Tunneling

Ilica Mahajan and Irene Manousiouthakis

Introduction:

In 1947, while Goos and Haenchen were investigating evanescent waves, they discovered an intriguing and unexpected displacement of a light beam. A bounded light beam experienced total internal reflection. This takes place when the beam of light strikes the boundary between two mediums, and the angle with which it strikes happens to be larger than the critical angle. This only occurs when the beam is passing from a medium of a higher refractive index to one with a lower refractive index. Today, this effect has several applications: fingerprint reading technology, fiber-optic communications, superconductivity, scanning tunneling microscopes, etc.

Another property of the evanescent wave is evident in Quantum Tunneling. In this phenomenon, a medium is present between two layers of another medium. A light beam is shot through a trajectory that passes through the first medium, then the second, and back to the first. The mediums could be, for example, clear plastic for the first medium, and air for the second medium. Surprisingly, instead of being reflected on the first medium's boundary, the light beam continues through. If the second outer region is not present, then the wave becomes totally reflected. So, at a certain point, if the gap between the two outer mediums becomes too large, the second medium is no longer able to "catch" the beam, and instead the light beam reflects as would be expected. This is an example of the evanescent wave coupling effect, and happens because Schrödinger's wave equation governs the behavior of particles. This is called tunneling since the beam "tunnels" through the second medium barrier.

Overview and Goal:

Since the Goos-Haenchen shift is too small (usually it is a fraction of the wavelength of the radiation) to be demonstrated by light, we will use microwaves with wavelengths of about 3 – 5 centimeters. It thus only takes a single reflection to see the effect as opposed to the hundreds of reflections that would be necessary to demonstrate the shift with normal light. We conducted a series of experiments to determine values for the Goos-Haenchen Shift and other properties of this effect. We used an emitter and a detector to determine where the waves are coming in, and then determine where they would be exiting the prism if the shift does not occur. We also investigated tunneling by measuring the distance at which the beam does not carry through the second prism. We will then draw conclusions with regards to the values and the experiment's setup and accuracy.

Materials

- Aluminum Foil
- Microwave Emitter
- Adjustable Stand
- Two 45˚ - 90˚ - 45˚ Plastic Prisms
- Wooden Guides
- Microwave Receiver Horn (Detector)
- Ruler

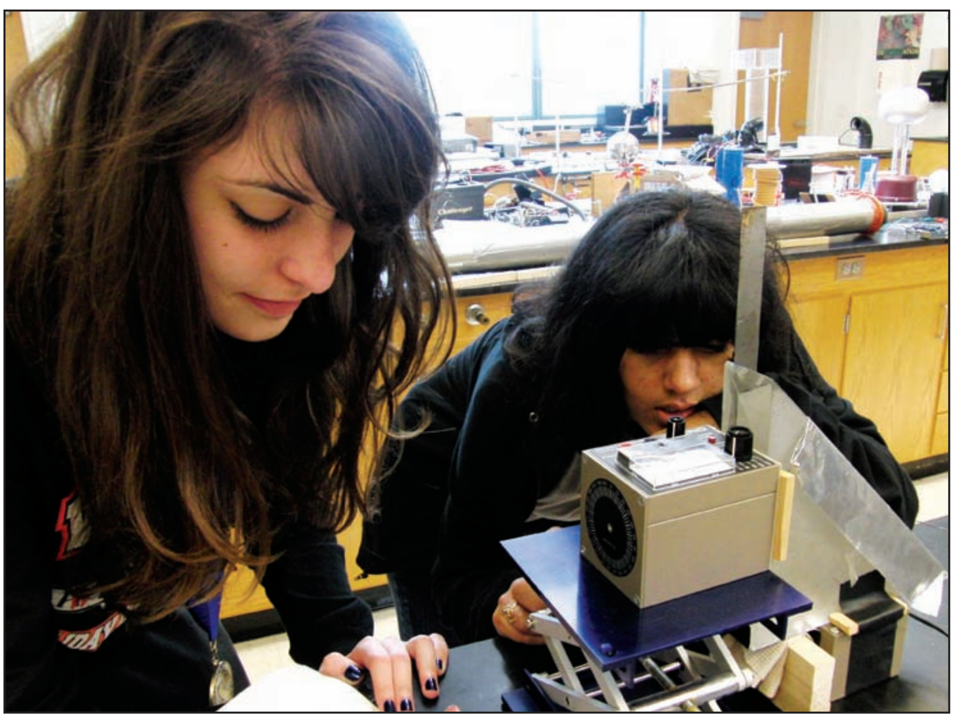

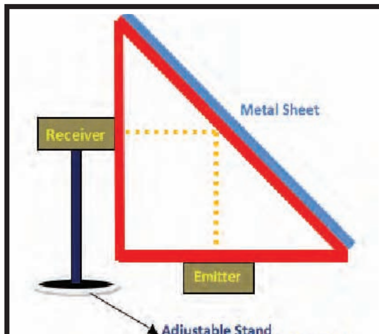

Figure 1

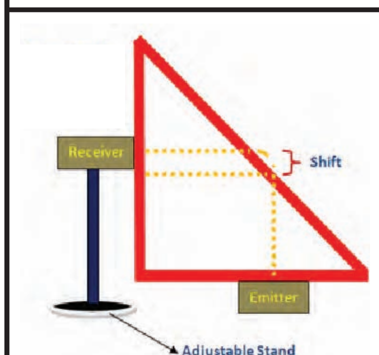

Figure 2

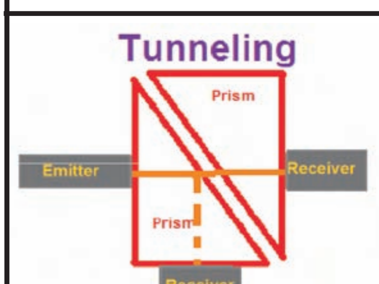

Figure 3

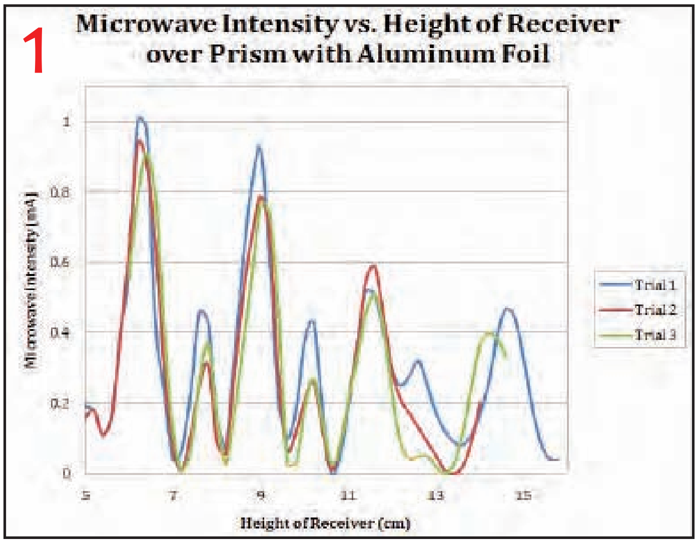

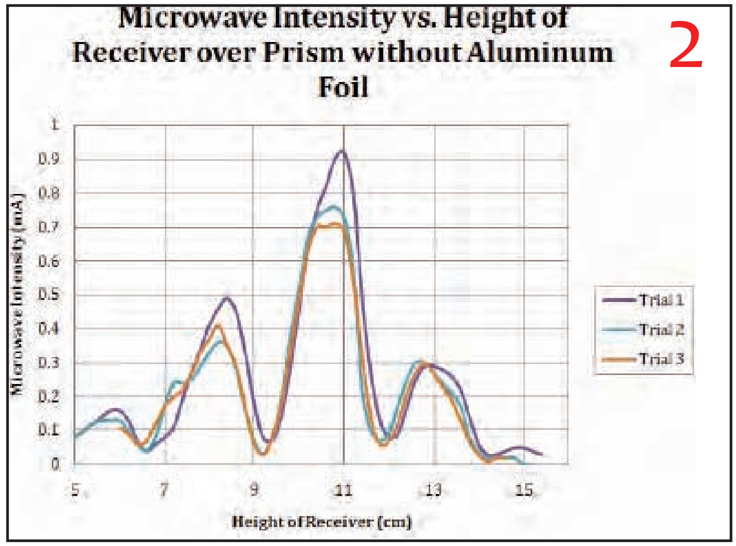

Method:

There were two main parts to the experiment: figuring out where the wave would exit in the absence of the evanescent property of waves and where it actually does exit. In order to prevent the shift from occurring, we approached the former problem by placing an aluminum sheet on the hypotenuse of the prism as shown by Figure 2. The rest of the setup is as displayed by the diagram, with the prism resting on an emitter, and a receiver placed on an adjustable stand and in contact with the side of the prism. We attached wooden guides to both the emitter and the receiver to ensure the same alignment each time, thus adding more accuracy to the figures we were measuring. We attached the ruler to the prism, making sure to align the 0 cm mark to the base of the prism. Since the aluminum sheet is a metal surface, it prevents the wave from exiting the prism. Thus, there will be no shift because the microwaves will be reflected.

In order to arrive at a figure for the location where the microwave is actually exiting the prism, we adjusted the receiver on the adjustable stand, taking data for every 0.2 cm that we moved the receiver starting a height of 5 cm above the base of the prism. We recorded the intensity as displayed by the receiver every 0.2 cm and then graphed this data. We repeated this with and without the foil and had 3 trials for each.

This time, according to Goos and Haenchen, there should be a shift. In other words, the strongest readings will not occur in the same place as when the metal sheet was present. We measured the distance from the bottom of the prism to the point. In order to determine the shift, we subtracted our earlier measurements with the metal sheet from this new measurement. Only the relative measurements are relative for determining the shift.

Finally, we performed some experiments on Quantum Tunneling. We took two 45˚- 90˚- 45˚ prisms and placed their hypotenuses close together (Figure 3). We measured the gaps between the prisms in order to determine the point at which the gap became so large that tunneling did not occur. We placed the receiver at the same height as the emitter on the other side of the two prisms and tried to detect the strength of the wave. We then recorded the values as we began to pull the two prisms apart. This confirmed that tunneling does not occur when the second prism is not present by removing the second prism and observing the reflected wave by placing the receiver at the base of the prism.

All of our measurements were handled as meticulously as possible. However, there were certain aspects of the experiment that were not under our control, and thus contributed to some error. In order to minimize error, we took three trials and averaged the values.

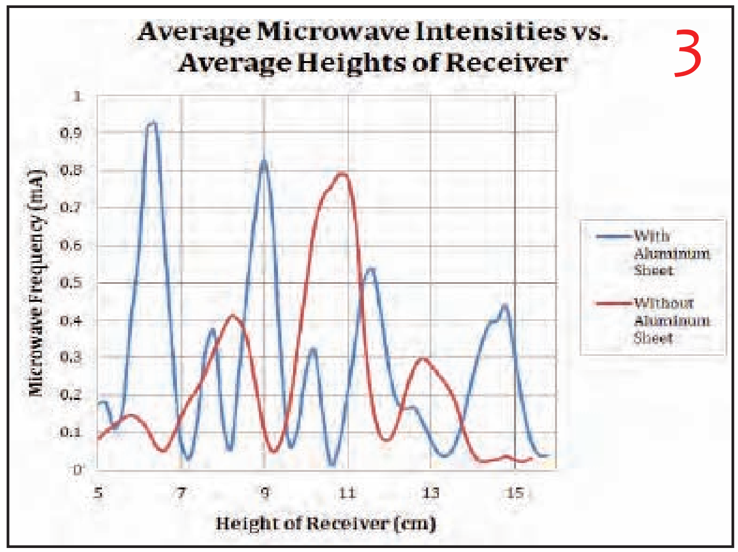

Conclusions:

By looking at the peaks of graph 3 for both microwave intensities, with and without the aluminum foil, we were able to determine the Goos-Haenchen Shift for the particular prism. The peak of the prism with the metal sheet, expected to have no shift, has a concentrated region of microwaves at a height of 6.267 cm. The peak of the prism without any interference has a peak at a height of 10.933 cm. Thus, by determining the difference in these heights, we obtained a shift of 4.666 cm. This seems like an acceptable figure considering the values should have been between 3-5 cm because the shift should be less than the wavelength of the microwaves. The reason for multiple peaks is due to the fact that the microwaves are reflecting within the prism at different angles. By looking at only the highest peak on the graph, we eliminate any confusion in the shift.

The set-up of our experiment may result in data that is highly susceptible to error. If the foil used to eliminate the shift isn't hugging the prism properly, then the wave would be allowed to exit until it hit the foil, which means there would be a slight shift. This means that the value we get might be smaller than the actual value. Even the simple readings on the receiver for intensity are not accurate enough to determine the most precise values for the max intensity. This could change where the shift occurs as we adjust the height of the receiver.

Harvesting Light for Energy

Rohun Bansal and Max Simchowitz

Due to the various shortcomings of conventional photovoltaics, we have decided to investigate a promising and somewhat elementary technique of reaping energy from sunlight – Quantum Dots. We have spent our time investing quantum dots as an electrodynamic harmonic oscillator. If time permits, we hope to use our simulation of a quantum dot to understand how multiple excitons can be generated.

Introduction:

Up until now, photovoltaic panels have consisted of rigid silicon layers that use incident light to dislodge electrons and generate current. Due to their cost, limited efficiency, and inflexibility, these cells have been extremely difficult to implement as a viable source of energy. Alternate compounds promise much greater efficiency, lower cost, and can be implemented in flexible plastics to be placed on cars, roofs, and ever consumer electronics.

Our project intends to investigate in a simple yet robust manner the scattering of electrons in a quantum dot attached to two wires so that we can better understand one of the most viable methods of harnessing solar energy. To accomplish this, we used a Mathematica package by Michael Trott, "Scattering of Scattering States in a 2D Quantum Dot Embedded in a Waveguide", which describes a circular quantum dot attached to two rectangular wires. We are attempting to adapt the package to visualize scattering in a spherical quantum fixed to two cylindrical wires. We believe that the spherical shape more realistically represents the quantum dot and could be more useful in testing its potential as a light harvesting compound.

Conventional Solar Cells:

Traditional silicon-based solar cells use two types of doped silicon, p- and n-type layered together. When an atom in the crystal lattice of the solar cell is struck by a photon of energy greater than its bandgap, an electron is given enough energy to leave the valance band and go into the conduction band, leaving a "hole" behind. Since there is as diode between the p-type and the n-type silicon, there is a favorable direction for the electron to travel (toward the n-type side) and another for the hole to travel (toward the p-type side). This process creates a current from the n-type side, which is transferred via metal contacts to a load and back to the p-type side, where the electrons recombine with holes. The problems with using this phenomena are that (1) photons of energy lower than the bandgap of the semiconductor used are not utilized and (2) that for photons of energy greater than the bandgap, the difference in energy between the photon and the bandgap is converted into heat via lattice vibrations rather than into usable electrical energy. Using multiple p-n junctions and different semiconductors (like GaAs and InP) can better match the solar spectra and can provide efficiency of conversion greater than 50%.

Quantum Dots:

Quantum dots have a tunable band gap, or a wavelength that can be absorbed. Various quantum dots can be mixed to absorb incident light at a full distribution of wavelengths. Quantum dots are also small enough to be placed onto flexible substrates and offer strong electronic coupling so that the excitons exist for long durations of time and can thus transmit large voltages. The tunable band gap also promises the implementation of "thermovoltaics", or the absorption of infrared radiation to generate current[1].

Quantum dots can also produce multiple excitons which, unlike in bulk semiconductors, don't dissipate due to heating. Thus the energy yield per photon and therefore efficiency as a whole can be increased. These excitons travel roughly near etched out crystal channels. These are the unique properties we wish to simulate on a quantum level to investigate the fundamental differences between conventional and novel materials.

Quantum dots can also be incorporated into the traditional silicon-based solar cell design by creating layers of quantum dots between the p- and n-type semiconductors. The quantum dots aid in converting longer wavelength light into usable electrical energy by lowering the effective bandgap for absorption. In addition, the quantum dots are able to collect the photoexcited charge carriers with high internal quantum efficiency and transfer the electrons and holes into the neighboring p- and n-regions with high efficiency. This translates into a higher operating efficiency and a higher short-circuit current with little expense to the open-circuit voltage[2].

Theory - Existing Package:

So far, we have been studying Mathematica, advanced electrodynamics, and elementary quantum mechanics through a pre-existing Mathematica package by Michael Trott: "Scattering States in a 2D quantum dot embedded in a wave guide"[i].

The package describes the motion of electrons moving from a left arm (with a certain reflective constant) through a quantum dot to a right arm (with a certain transmittance constant).

Figure C is a representation of the domain which the existing package solves for, with the quantum dot in the center represented as a circular region and the two arms represented as rectangular regions. Because electrons behave as waves in this medium, the set up can be treated as a vibrating membrane. Thus, the package uses a Helmholtz solution for harmonics across a fixed membrane to model electrons' motions. We truncate the infinite summation of these quantities at p, q, and o for simplicity.

See Equation Set A, for the equations for thet left arm, the quantum dot and the right arm.

Each of the three equations is dependent upon a mode upon which the wave number Km (in the arm Helmoltzs equations) and the Bessel Function value Jm (in the quantum dot) rely. The package then designates αk, βk, γk beta, and gamma coefficients for each wavenumber as a certain ck value:

Modifications and Problems:

$$c_1,\ldots,c_p \equiv \alpha_1,\ldots,\alpha_p \text{ (leftarm)}$$
$$c_{p+1},\ldots,c_{p+q} \equiv \gamma_1,\ldots,\gamma_p \text{ (rightarm)}$$
$$c_{p+q+1},\ldots,c_{p+q+o+1} \equiv \beta_0,\ldots,\beta_{o+1} \text{ (centerdisk)}$$

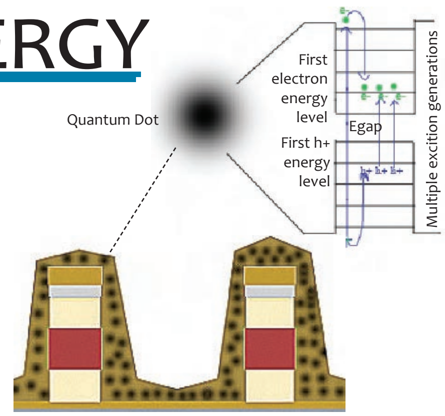

A diagram (top) details the state of an electron at varying levels of excitement in a quantum dot. A schematic (bottom) shows the trenches cut into the layered semiconductor.

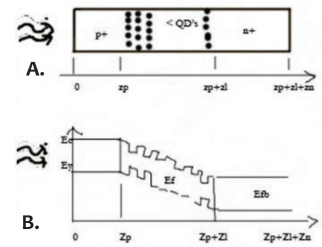

Fig. A:
Schematic structure of a quantum dot solar cell.

Fig. B:
Energy-band diagram of p-i-n quantum dot solar cell, showing the p+- type layer, intrinsic layer with quantum dots, and n+ - type layer.

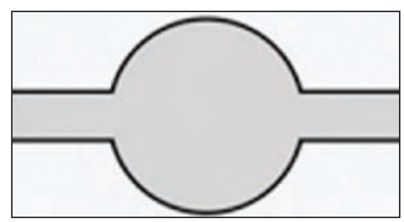

Fig. C:
The domain that the equation package solves for, with the quantum dot at the center and the arms extending to the sides.

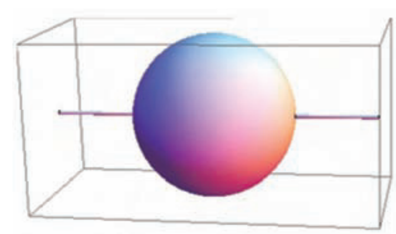

Fig. D:
Bansal and Simchowitz are attempting to solve for the domain of a quantum dot-on-a-wire, represented above.

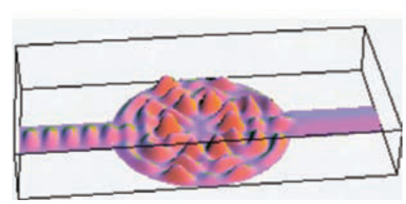

Fig. E:
Bansal and Simchowitz are attempting to solve for another domain of a quantum dot-on-a-wire, represented above.

Left arm: $\psi(x,y) = e^{ik_1 x} + \sum_{m=1}^{\infty} \alpha_m e^{-ik_m x} \cos\left(\frac{(2m-1)\pi y}{L}\right) \approx e^{ik_1 x} + \sum_{m=1}^{n} \alpha_m e^{-ik_m x} \cos\left(\frac{(2m-1)\pi y}{L}\right) = \xrightarrow[x\to-\infty]{} (e^{ik_1 x} + R e^{-ik_1 x}) \cos\left(\frac{\pi y}{Ly}\right) \cos\left(\frac{\pi z}{Lz}\right)$

Quantum Dot: $\psi(r,\varphi) = \sum_{m=0}^{\infty} \beta_m \cos(m\varphi) J_m\left(\sqrt{\mathcal{E}} r\right) \approx \sum_{m=0}^{n} \beta_m \cos(m\varphi) J_m\left(\sqrt{\mathcal{E}} r\right)$

Right arm: $\psi(x,y) = \sum_{m=1}^{\infty} \gamma_m e^{ik_m x} \cos\left(\frac{(2m-1)\pi y}{L}\right) \approx \sum_{m=1}^{q} \gamma_m e^{ik_m x} \cos\left(\frac{(2m-1)\pi y}{L}\right) == \xrightarrow[x\to\infty]{} T e^{ik_1 x} \cos\left(\frac{\pi y}{L}\right)$

Equation Set A:

If we treat the central as a spherical oscillator, we can represent its Helmholtz Equation as:

In our three-dimensional model, the left

$$A(r,\theta,\varphi) = \sum_{\ell=0}^{\infty} \sum_{m=-\ell}^{\ell} (a_{\ell m} j_\ell(kr) + b_{\ell m} y_\ell(kr)) Y_\ell^m(\theta,\varphi)$$

and right arms are cylindrical waveguides, not vibrating membranes. The wires still have length L, but now have a separate radius of their own. For the central sphere, whereas in the existing package the coordinate system was modeled with a simple theta-r polar coordinate system (with r ranging from 0 to the outer radius R and theta = 0 being at the midpoint of the right arm), in our 3D adaptation we introduce a new variable – phi (an angle perpendicular to theta) – to create a spherical coordinate system.

Figure D is a representation of the quantum dot-on-a-wire domain that we are attempting to solve for. Note the two cylindrical arms on both sides and the spherical quantum dot in the center. Inside the quantum dot are shells of which we aim to graph the solutions on. However, we have yet to find a Helmoltz equation that would represent this situation.

The difficulty is that these two equations, because of their higher dimensionality, have two wave numbers – l and m. These require more sophisticated symmetry and boundary conditions. Moreover, these functions are represented across yet another angular dimension, phi. To resolve these issues, we would need the assistance of a professor working in the field. However, we can model a spherical quantum dot in isolation using the wave function for an isotropic quantum oscillator and graph it using techniques illustrated later.

In this function, Lkl+1/2 represents the

$$\psi_{klm}(r,\theta,\phi) = N_{kl} r^l e^{-\nu r^2} L_k^{(l+\frac{1}{2})}(2\nu r^2) Y_{lm}(\theta,\phi)$$

Laguerre polynomial, defined by
and Nkl is the normalization constant defined by

$$L_n^{(\alpha)}(x) = \sum_{i=0}^{n} (-1)^i \binom{n+\alpha}{n-i} \frac{x^i}{i!}$$

The waves k,l, and m represent the different modes

$$N_{kl} = \sqrt{\sqrt{\frac{2\nu^3}{\pi}} \frac{2^{k+2l+3}\, k!\, \nu^l}{(2k+2l+1)!!}}$$

of the wave: the energy number "n" is defined by 2l+k, and m is an integer on the interval [-l,l]. Because of the relationship between k, l and m, the Wolfram Isotropic Quantum Oscillator demonstration represents the wave function of the particle as $\psi_{nlm}(r,\theta,\phi) = R_{nl}(r) Y_{lm}(\theta,\phi)$

where $R_{nl}(r=) N_{nl}\, r^l e^{-\omega r^2/2}\, L_{(n-l)/2}^{l+1/2}(\omega r^2)$. For our project, we will use this representation of the wave function.

Fourier Constant Calculations:

The solution tables:

The continuity functions calculate the Fourier coefficients for a valid solution. After this point, the program generates two matrices to represent a system: a left hand side matrix representing variables for the different coefficients and a right hand side matrix with their answer to each. The program then finds the pseudo inverse of the left hand side, and multiplies that quantity by the right hand side matrix, essentially solving the system and attaining a matrix of constants for αk, βk, γk. These are then used to create the wave function definition.

Because this process was created for only one wave number, it needs to be drastically revised to accommodate our two wave number three dimensional adaptation. In our simplified spherical quantum dot representation , the constants are already provided. However, for the sake of efficiency, we will create a table of all the normalization constants before graphing the wave function so that similar calculations are not repeated.

Graphs:

The scattering plot graph in the original version uses Mathematica's Polygon [points_] function which turns a set of points into a diagram with rendered polygons. For every point at (x, y), the program renders a point above the graph at coordinate z that corresponds to the value of the wave function, z = ψ(x, y), at that point. The resulting image is Figure E.

Because our graphs are limited to three dimensions, representing scattering states in a three dimensional system is more difficult to represent. Here we encounter the aforementioned problem that our spherical Hemholtz equation has three parameters, but we can only represent two. Thus, we need to plot the scattering states on a flat surface, i.e. in a plot where one variable is written as a function as of the other two. There are two intuitive ways to do this:

The first would be to represent scattering on a flat cross section of the quantum dot at a constant z coordinate. Thus we would plot Cartesian wave function ψ(x, y, n), or our spherical wavefunction ψ(r,θ,α), for a constant n = sin α. Without the scattering plot, Figure F is how one such cross-section would look.

The second way to visualize scattering would be draw it on a spheroidal shell based on a constant c from 1to infinity (becoming narrower as c increases).

In this case, we would plot Cartesian wave function ψ(x, y, z) where $z = \pm\frac{1}{c}\sqrt{R^2 - x^2 - (cy)^2}$

for $x \in (-R, R)$ and $y \in (-\frac{\sqrt{R^2-x^2}}{c}, \frac{\sqrt{R^2-x^2}}{c})$.

This would be more difficult, because the y, and z coordinates of the polygon depend on both the actual y and z coordinates inputted into the wavefunction and the value of the wave function itself. Thus, to find the y and z coordinates in the shell representation, we need consider a vector of magnitude ψ(x,y,z) pointing in the same direction as a vector beginning at the (x,o,o) and ending at (x,y,z), which we may call ψ. Thus (x,y,z)point = (x , y + ||ψy (x,y,z)|| , z + ||ψz(x,y,z)||), where ||ψy(x,y,z)|| = cos(arctan(z/y)) and ||ψz(x,y,z)|| = sin(arctan(z/y)).

We plan to project the function onto plots of the shapes in Figure G, representing different "shells" within the structure, progressing from the outermost to the innermost (c = 1.2, 1.5, 2).

Conclusion:

We have yet to generate a suitable 3-D adaptation to right a conclusion. However, we anticipate that the 2-D quantum dot set up will end up being a reasonably approximation of the 3-D system.

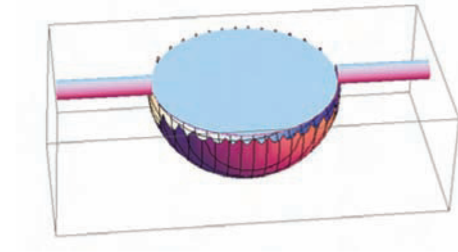

Fig. F:
This plot represents Cartesian wave function for a constante n=sin α.

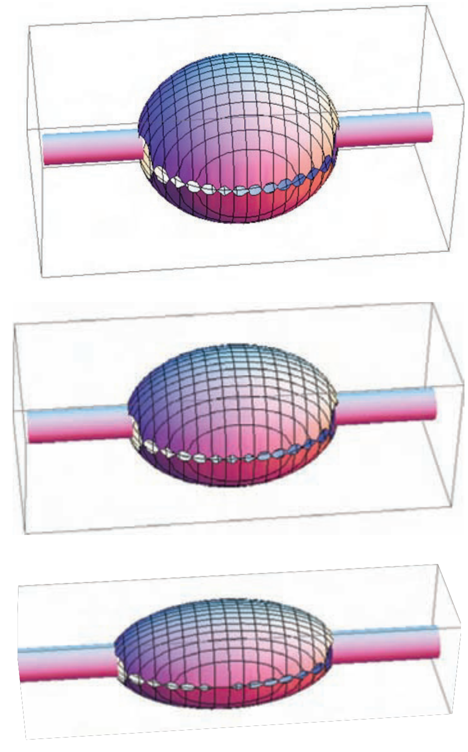

Fig. G:
Bansal and Simchowitz plan to project the Cartesian wave function onto the three above shapes, representing different "shells" within the structure, progressing from top to bottom, c=1.2, c=1.5, and c=2.

1. http://www.i-sis.org.uk/QDAUESC.php
2. http://www.esqsec.unibe.ch/pub_89.htm: Quantum Dot Solar Cells, V. Aroutionian, S. Petrosyan, A. Khachatryan, K. Touryan*
i. Trott, Michael. Scattering States in a 2D Quantum Dot Embedded in a Waveguide. The Mathematica Journal. Volume 10 Issue 1. 2006.

The Paradox of Chilling Water

Two seniors investigate the **Mpemba** effect to find why water at different temperatures **cools** at **different rates.**

Andrew Wang and Monica Chen

Background:

Water defies simple logic. The two hydrogen-one oxygen compound residing in all organic life forms, the stuff covering 70% of our planet, and the substance we continually search for, water is considered the most standard of fluids and has been vastly studied, yet remains an unsolved puzzle. What's more, due to the frequent use of water in various industries, all aspects of water, from reverse osmosis properties to hydrolysis, are crucial foci of research. In particular, this article is a report on recent efforts to investigate what has been commonly coined as the Mpemba effect. However, instead of focusing on the aspect of freezing, we thoroughly demonstrate in controlled environments the varying speeds at which differing temperatures of water cool.

While there are archives suggesting that ancient scientists dating back to Aristotle have observed the freezing of warmer water faster than cold water, only in recent modern times has such a phenomenon been experimentally detailed. In 1963, Erasto B. Mpemba noticed that his hot ice cream mix froze faster than the cold mixes. From that discovery, a number of successive experiments have replicated such results, albeit still unable to fully understand the underlying mechanism. Mainly, the wide variety of possible variables would require an unprecedented amount of experiments to establish not only the relation of each variable to the experiment but also the possibility of variable dependency. As such, most research in the area has been stagnant and primarily a focus on the validity of warm water freezing faster than hot water.

In comparison, our research focuses not on the point at which differing temperatures of water freeze, but rather, the process of cooling for "warm" and "cold" water. Our report investigates the rates at which hot and cold water cool and the point at which hot water evidently reaches a lower temperature than cold water in the same amount of time. Based on the starting initial temperatures, we establish consistently a temperature value in which hot water temperatures reach the same temperatures as cold water. Therefore, we assert in this report that hot water indeed cools faster than cold water and for every specific set of hot and cold water temperatures there is a consistent constant at which the cooling of hot water overtakes cold water.

While most objections to the validity of the phenomenon include the potential significance of environmental factors, our use of vacuums for cooling eliminates such concerns. Using a vacuum to lower the pressure of the atmosphere above the water sample, we can essentially cause the liquid to boil once the atmospheric pressure has reduced to that required of the liquid's phase graph. As a result, the "hottest" molecules in the water (those with the most kinetic energy) gain the necessary momentum to escape from the bonds of the compound into the atmosphere. Thus, the average temperature of the water will slowly drop as the pressure continues to decrease continuously as the molecules with greater kinetic energy become water vapor. However, the most significance lies in the ability to eliminate environmental factors due to the vacuum. Thus, we are able to examine this effect by controlling specific variables.

Method and Procedure:

To begin the experiment, first set up the apparatus. To do so, first fill a large beaker with an ice-water mixture. Next, fill one 200 mL beakers with 30 mL of double-distilled water. Drop a magnet stirrer into the beaker and then place the beaker on the hot plate. Set the heat dial to two and the stirring dial to 3. Place an electronic thermometer into the beaker and leave the beaker on the hot plate until it reaches 40 degrees Celsius. Meanwhile, fill an empty 200 mL beaker with 15 mL of double-distilled water. Place an electronic thermometer into the beaker and then place the beaker into the large beaker filled with ice-water prepared previously for 2 ½ minutes or until the thermometer reads 5 degrees Celsius.

While waiting for the beakers to reach the correct temperatures, fill the vacuum with oil so that it is operable. Then, apply the lubricating grease on the platform of the bell jar.

Once the "hot" beaker has reached 40 degrees Celsius, pour 15 mL of the water into a graduated cylinder. Dump the excess water into the sink and then pour the 15 mL into the empty beaker.

After the "cold" beaker has been sufficiently cooled, remove the beaker from the ice-cold mixture and wipe away any ice that might have clung to the beaker.

Place both 200 mL beakers with their respective thermometers into the vacuum and attach the cord connecting the vacuum to the bell jar and put on the bell jar top. When the apparatus is ready and the approximate temperatures are 35 and 5 degrees, turn on the vacuum and start the timer.

Take temperature readings for both beakers every 30 seconds for 10-15 minutes.

Within the first three minutes, the water should begin boiling. Observe the discrepancy in the boiling rate in the two beakers. The beaker that initially had warmer water should cool faster.

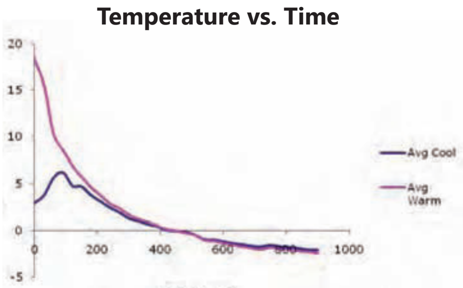

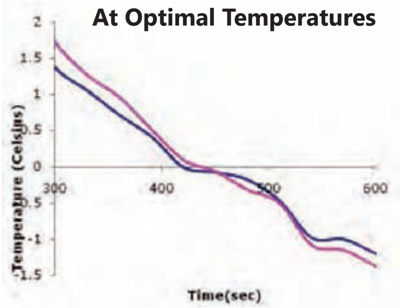

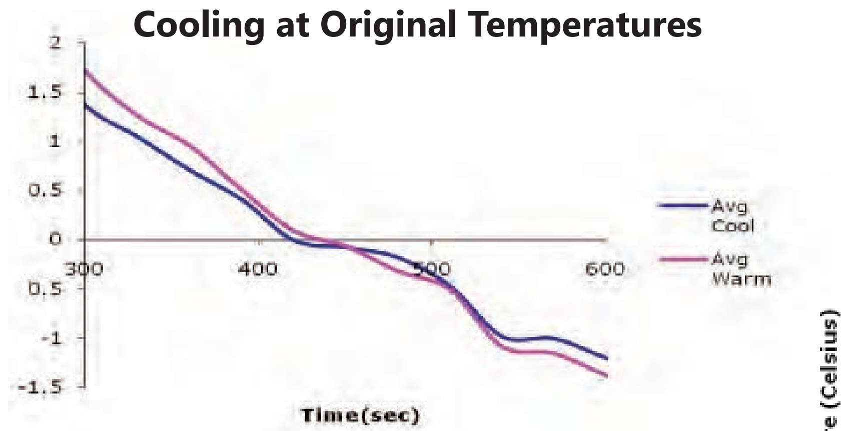

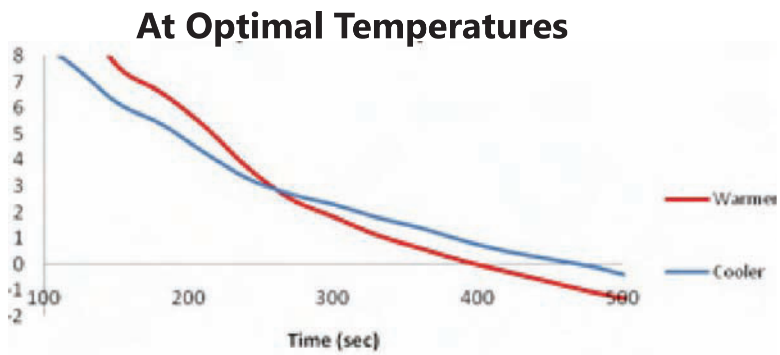

The two smaller graphs above show the disparity between warm and cold water cooling beginning at 17 and 20 degrees Celsius (above). Optimal temperatures for cooling begin at 35 degrees and 5 degrees Celsius (below). At right, magnifications of the sections of the above graphs that show the intersection of the warm and cold water cooling rates.

Data and Results:

The data collected can be broken into two groups: data collected at the optimal temperatures suggested by New Scientist to maximize the Mpemba effect and data collected at room temperature and a randomly selected temperature between [Figure 1 and Figure 2 respectively].

There are three important areas of the graph: the initial section, right before the crossover, and the point of crossover.

In this first graph, we choose the set where the "hot" water temperature is at around room temperature and the "cold" water is at around 3 degrees. The warm water begins to cool immediately, progressing rapidly after it begins to boil at roughly t=25 seconds. In comparison, the cold water equilibrates to room temperature until it begins to boil at roughly t=90 seconds whereupon it begins to rapidly cool. After t=200 seconds, the two temperatures begin to converge. The experimental data ends a few minutes after the point of cross over.

As the warmer temperature water begins to cool, it reaches a point (in this case t is around 450 seconds) where both temperatures are equal to each other. Our experimental data has this crossover point at slightly subzero Celsius.

As shown by New Scientist, the optimum temperature for the Mpemba effect is 35 degrees Celsius and 5 degrees Celsius. Accordingly, we have also examined such temperatures in comparison to our previously chosen temperatures. The warm water begins to boil almost instantaneously while the colder water boils at around t=100 seconds. The cross over happens at a lower temperature and the divergence of the two trend lines are far more apparent.

A close up magnification shows clearly a much more negative slop for the hot water than the cold water and in comparison to the temperatures previously used, optimize the result of hot water cooling faster than cold water.

Analysis and Discussion:

We have established that room temperature/hot water indeed freezes faster than cold water. From the results, one can conclude that the starting temperature does affect the crossover time where the initially warmer water becomes cooler than the initally cooler water. When using the "optimal temperature" data, the crossover time is at 490 sec. On the other hand, the crossover time using the other set of data is at 250 seconds, a considerably shorter time than when using the optimal data. This illustrates that temperature does have an affect on the crossover time.

The warmer water's temperature rapidly decreases due to the combined effect of adjusting to room temperature and the vacuum.

The cooler water's temperature on the other hand initially increases as it acclimates to room temperature. When the vacuum's effect kicks in, the temperature peaks and immediately starts to drop.

One interesting point to note is that the crossover temperature also differs between the two sets of data. Using the optimal temperatures, the crossover occurs at 2.7 degrees C while the crossover occurs at -1.3 degrees C in the other set of data. We will continue to investigate this point in the coming weeks to determine exactly why this occurs.

Furthermore, it is also observed that room temperature water boils slightly faster than cold water. While the latter initially seems logical, the rate at which the vacuum pump decreases the surrounding air pressure is quick enough such that the difference in liquid temperature should result in little to no disparity of boiling timing. As mentioned in the introduction, many theories, all of which have no strong explanation, have plagued this strange occurrence. The evaporation theory, which suggests that mass loss results in faster freezing, is not significant due to the mass of water loss. In the same way, there exists an idea that there are less dissolved gases in hotter water, but there is no theoretical or experimental correlation. Finally, while the environmental change theory is nearly impossible to observe or explain, the convection current theory remains the most plausible, yet is still not entirely clear. Though water at the top may be hotter at the top and also cooled before the bottom liquid, this would also be highly dependent upon the container used.

Conclusion:

In the end, what we conclude is simple and succinct: hot water cools faster than cold water. Obviously, with enough time and effort, the cooling rate of water from temperatures between zero and 100 Celsius could be examined, giving us a relationship dictating the rate at with water cools.

Acoustically Creating the *Casimir Effect* with an *Oscillator*

Daniel Lundberg

Purpose:

The purpose of this experiment is to create attractive or repulsive forces between two plates through the Casimir Effect using acoustic energy and to determine what types of noise are most efficient.

Original Experiment:

Two plates are positioned close to each other in an enclosed environment full of acoustically reflective surfaces, and noise is produced from a precise loudspeaker tweeter to create Casimir forces based on the distance between the plates and the wavelengths associated with the distances.

Pink noise is equalized to include peaks at the standing wave frequency and its harmonics, and movement of the plates resulting from the acoustical stimulation is observed and recorded.

Initially, frequency response traces were taken of the first tweeter reproducing these different types of noises, and it was concluded that the combination of the amp and tweeter created too much harmonic distortion (THD) to accurately reproduce the noises being sent.

A self-powered speaker with flat frequency and phase response was obtained to replace this. No usable data was obtained with the plates parallel to the sound waves, so the plates were repositioned to be perpendicular and a high-speed video was made.

Analysis:

When the noise was played, the two plates each moved away from the speaker by slightly different amounts. It is difficult to definitively state the cause of the movement or express it mathematically, but several factors can be ruled out.

The plates did not move because of acoustic pressure, because movement based purely on the pressure changes caused by the tweeter's oscillation would respond to both compressions and rarefactions, and the plates never swung towards the speaker from their equilibrium position as they would have in an oscillation.

Furthermore, what would have been the period of oscillation of the plates was far below the periods of the frequencies being played back, with all of those frequencies existing above 2 kHz (2000 cycles per second). The movement of the plates was not caused by external forces because it occurred in an enclosed environment and began exactly when the noise did.

The movement could have been caused by differences in the amplitude of the noise, so a better result could be achieved by using a more consistent noise generator. Because of the weight of the plates compared to the microscopic Casimir forces, this experiment would be better served by using lighter materials, rigging methods with less friction, or possibly a different medium altogether, such as water.

Revised Method:

New, smaller plates made out of a thin plastic are suspended by thread from a rigging mechanism that can easily adjust the distance between the two plates and lowered into a beaker of water that is placed on top of a shaker. The shaker is a large speaker cone filled with foam providing a flat surface to respond to the oscillations of the cone caused by the oscillator. This was originally tried with a larger water container and larger metal plates, but this set up proved too massive for the shaker to produce the Casmir force between the two plates.

Data:

High-speed videos were made of the oscillator making sine, square, and triangle waves at a frequency of 10.5 Hz:

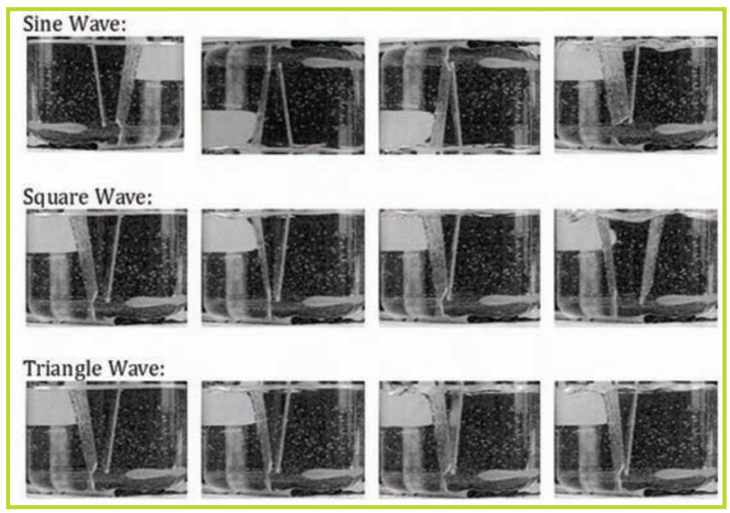

Final Analysis:

The plates' movement is drastic and can only be explained by the Casimir effect. The movement of the plates varied with the amplitude of the oscillator and with time, and sine waves seemed to be the most efficient means of creating attraction with square waves being the worst. Plates also separated with increased amplitude; it is unclear if this is purely because of the overpowering of outside forces or if there is a repulsive force involved.

Conclusion:

This experiment will benefit from precisely measuring the distance between the plates and the amplitude of the signal.

As the distance between the plates changes as they come together, it is impossible to pick one frequency that will stimulate the greatest force, so further experimentation will include trying different frequencies related to the distance between the plates and also trying multiple frequencies and Brownian (low frequency) noise.

INVESTIGATING *MAGNETIC ACCELERATION*

Charlie Fogarty

Magnetic acceleration is closely associated with Newton's first law; for every action there is an equal but opposite reaction. As demonstrated in the novelty Newton Clacker, the energy of the first swinging steel ball is transferred to the last steel ball. The magnetic acceleration demonstration introduces a neodymium magnet into the equation and places the system on a track. The neodymium magnet has three ball bearings on one side. Another ball bearing is released on the other side of the magnet and as it rolls down the track it collides with the magnet causing the energy from the first ball bearing and the energy from the magnetic attraction to be transferred to the last ball bearing on the other side, causing it to accelerate away from the system with significantly more energy than the first ball bearing.

My research is focused on the idea of a critical velocity of the first ball bearing that causes the greatest difference between energy input vs. energy output.

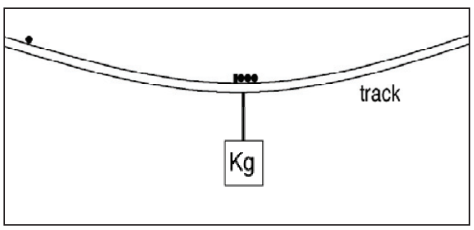

Figure 1: The basic set up with bent aluminium track, magnet and ball barings.

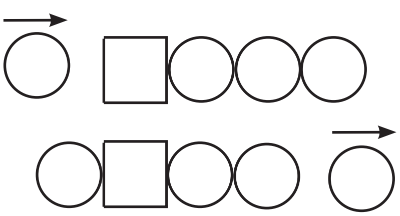

Procedure:

I conducted my tests on a parabolic track to more easily measure the distance the front ball bearing traveled from the magnet. I have bent the track by hanging a constant weight from the center of an aluminum v-shaped bar. I used a 1/2" x 3/16" N42 Neodymium disk magnet, and four 1/2" nickel-plated steel balls. I set up the neodymium magnet with three steel balls to one side. The middle two balls act as spacers so the fourth ball (front ball) is only weakly attracted to the magnet. Another steel ball of the same size and mass is then released so it collides with the opposite side of the magnet.

I released the ball bearing at centimeter and ten-centimeter intervals from the magnet, and recorded the distance the accelerating ball traveled. For each interval I performed three trials and took the average of the distances.

Results:

By carefully recording the distance from the magnet the first ball bearing was released, and the distance the last ball traveled from its staring point, I made this graph showing the differences of D1: distance ball 1 was released, and D2: distance ball 4 traveled.

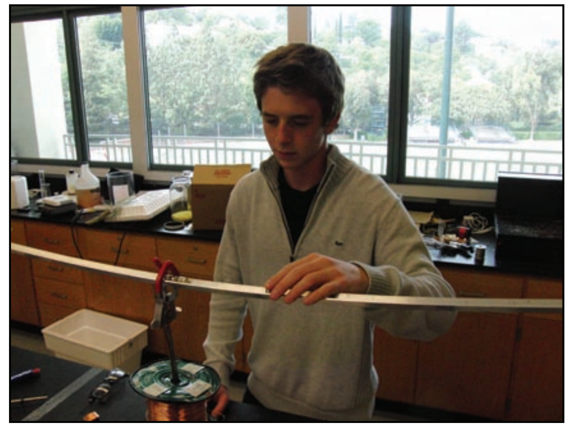

Conclusion:

Since this experiment was conducted on a symmetrical parabolic track we can assume the same bend and height on each side, and since the magnet/ball system was placed at the equilibrium point on the track, I believe that the distance ball 1 was released and the distance ball 2 traveled are equal to the energy in and energy out. What this graph then shows is: first, that the relationship between distance released and distance traveled is highly non-linear. The sum of the distance released and approximately 84 cm is significantly more than the actual distance traveled by the fourth ball. Second, and most importantly, the fact that the difference of D1 and D2 increases from 1 – 5 cm and then decreases from 6 cm to 100 cm shows that the magnetic acceleration is most effective when ball 1 is released from about 4-6 cm. Essentially, where there is the smallest proportion of energy input to output.

My results seem to suggest that the farther and higher ball 1 is released the less affective the acceleration is or the less affective the transfer of energy is from the ball 1 to ball 4. I increased the release distance from 1 to 100 cm and only measured a 17.5 cm increases in the distance traveled by ball 4.

One possible explanation for this is the idea of a critical velocity that yields the most effective acceleration. When ball 1 is released 5 cm from the magnet almost all of its collision force is caused by the magnetic attraction, accelerating the ball to a certain fast velocity (lets call it X), which in turn causes ball 4 to accelerate away with a similar velocity. When ball 1 is released from 100 cm away it enters the magnetic field with an initial velocity, and the magnet accelerates the ball to only slightly above velocity X. Newton's law of action and reaction stays true, but I believe the magnet is exerting slightly less force on the speeding ball (released from 100 cm) than on the almost stationary ball (released from 5 cm), and therefore causing the differences between D1 and D2 to get smaller the farther away ball 1 is released.

The major source of error in this experiment was friction between the ball bearings and the track. A way to fix this is to replace the magnet with a piece of metal the same size and mass and measure D1 and D2 to get control data.

In conclusion, there seems to be a tremendous amount of physics and magnetic science that takes place in this demonstration, and so far I have obtained solid evidence suggesting a critical velocity for the most effective magnetic acceleration, however, I would like to continue my research to answer the question with more specificity.

The difference of distance traveled by ball 1 and by ball 4

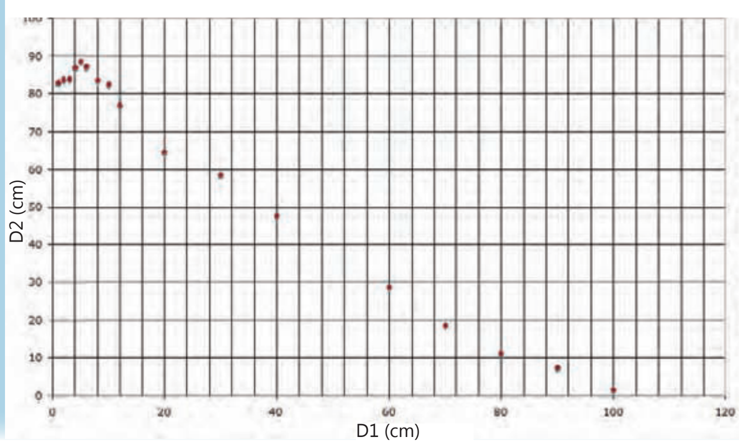

D1 (cm)	D2 (cm)
1	84
2	85.8
3	87
4	91
5	93.7
6	93.3
8	91.7
10	92.6
12	89
20	84.7
30	88.7
40	87.6
60	88.8
70	88.7
80	91.3
90	97.3
100	101.5

Making
Lightning

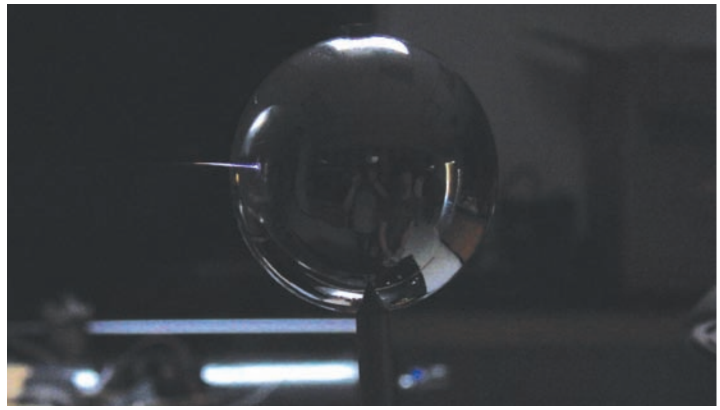

Riley Mate, John Billingsley and Matthew Krisiloff

Lightning has fascinated mankind throughout all of history, from the lightning hurled by the mighty Zeus at the ancient Greeks to the lightning bolts adorning the uniforms of the San Diego Chargers. As humans, we three share this fascination and we decided to explore and dissect a lightning bolt.

We thought that the best way to do this would be to bring the lightning down to a smaller scale and slow it down. In order to do this we obtained a Van de Graaff generator, and a high-speed camera that is able to shoot up to 1,000 frames per second and shoot 40 still pictures per second.

Our intention was to study the fractal patterns of the sparks induced by the generator. A question we aimed to answer was if the size and/or shape of the fractal are dependent on the size of the negative sphere of the Van de Graaff generator. We purchased three metals spheres of different sizes, ranging from two inches in diameter to four inches in diameter. We then drilled holes in each of the spheres that enabled us to safely fix them to the generator. We attached the smallest ball to the generator and proceeded to take high-speed movies and sequence shots of the sparks. This same procedure was done with the two other balls and we examined the movies and pictures we obtained.

The Van de Graaff generator can effectively simulate lightning originating from the clouds that moves down to strike the earth. The larger, positively charged ball induces a charge in the smaller ball through electrostatic forces. There is a belt under the larger ball that tears electrons away from the material of the belt, and deposits them on the large ball. The electrons from the large ball induce a charge in the smaller ball. Eventually these forces become so strong that electrons arc from one ball to complete the circuit on the other ball and release the built up electric potential energy.

Using our high-speed camera, we can view this "lightning" as it discharges between the two balls. Because of the infrequency of lightning in California, and the unpredictable nature of lighting itself, using the Van de Graaff generator, we can easily photograph lightning to learn more about its properties.

It is known that lightning discharges take place from the positively charged ground, and actually discharge upward into the clouds. The lightning we see in the sky is known as the "return stroke" and is a powerful discharge that proceeds the initial circuit completion between the negative and positive streamers. In our experiment, the large ball represents the earth, and the small ball is representative of the clouds. Using a high-speed camera, we are able to capture several lightning strikes between the two balls.

Our original experiment was to examine the fractal nature of lightning strikes between the two balls. However during one sequence we captured an event rarely seen. In the first image we can view the streamer coming off the smaller ball searching for the path of least resistance to complete the circuit to the larger ball. As the streamer moves further away from the first ball, the energy levels inside the streamer have a visual decrees in energy as seen by the different colorations of segments of the streamer.

This is a phenomenon that, to our knowledge has never been photographed before.

The second picture shows the complete circuit discharging from the larger ball and flowing back to the smaller ball as a return stroke. The tip of the lightning bolt is sharp, but the entire bolt is blue in color, the most likely explanation for this would be because the circuit has been completed, the voltage across the entire airspace remains constant, and therefore the energy output from the discharge will also be constant.

Through analysis of this image, we are able to witness an event only Zeus himself has ever had the pleasure of seeing. We believe this picture to be photographic evidence as to the reason of lightning's upward travel.

We were very lucky to even recognize the potential in this image, as many sequences of lightning strikes were deleted before making this discovery.

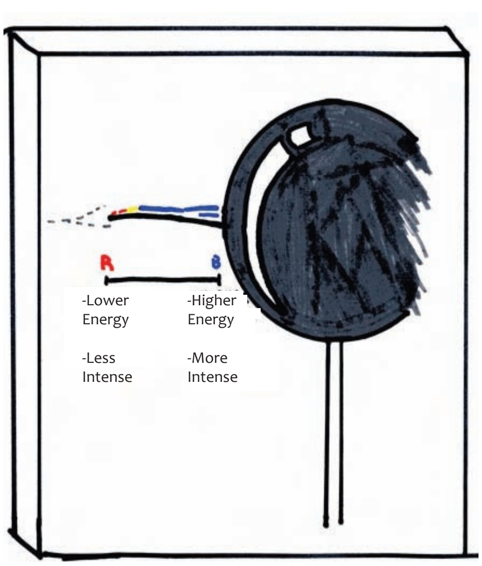

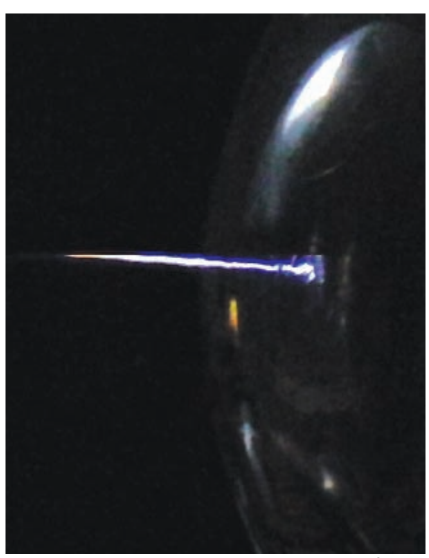

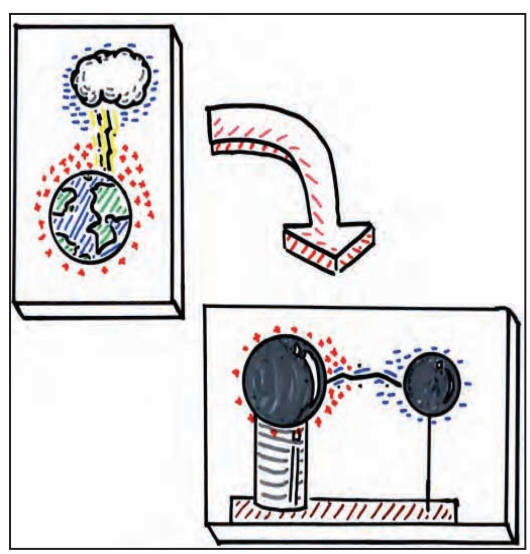

Diagrams and picture of how a Van de Graaff generator simulates ilghtning (above).

Creating a Vortex Ring Collision

Matt Girard and Ryan Plueger

Abstract:

Vortex rings are formed due to a complex combination of friction and pressure. The rings that are formed are very stable and maintain their ring-like shape in either water or air (in a smoke form). Rings keep their structure due to centripetal forces. In previous experiments, scientists have proven that colliding vortex rings create an intricate pattern if they collide perfectly. We will be creating a control chamber, wherein we will be building a small scale smoke ring machine.

Once we have built this machine, we will coat the inside of the machine with a metal material so that we can try and charge the smoke particles.

We will shoot the charged smoke ring towards a charged zinc metal sheet, hopefully seeing a difference in velocity of the ring. We are trying to observe whether or not it is possible to slow down the smoke ring through repulsion.

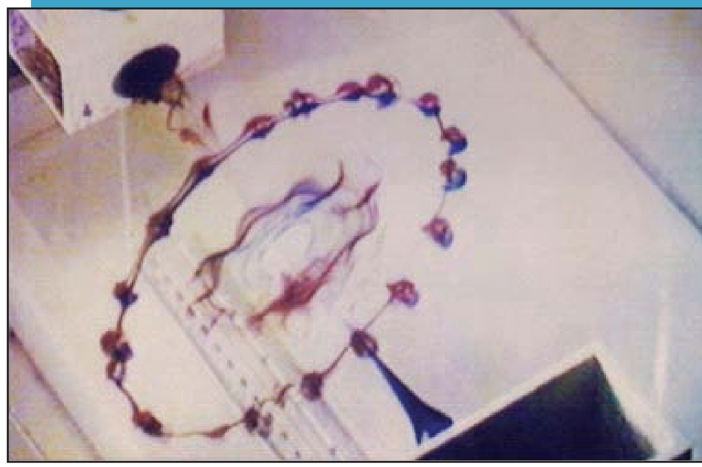

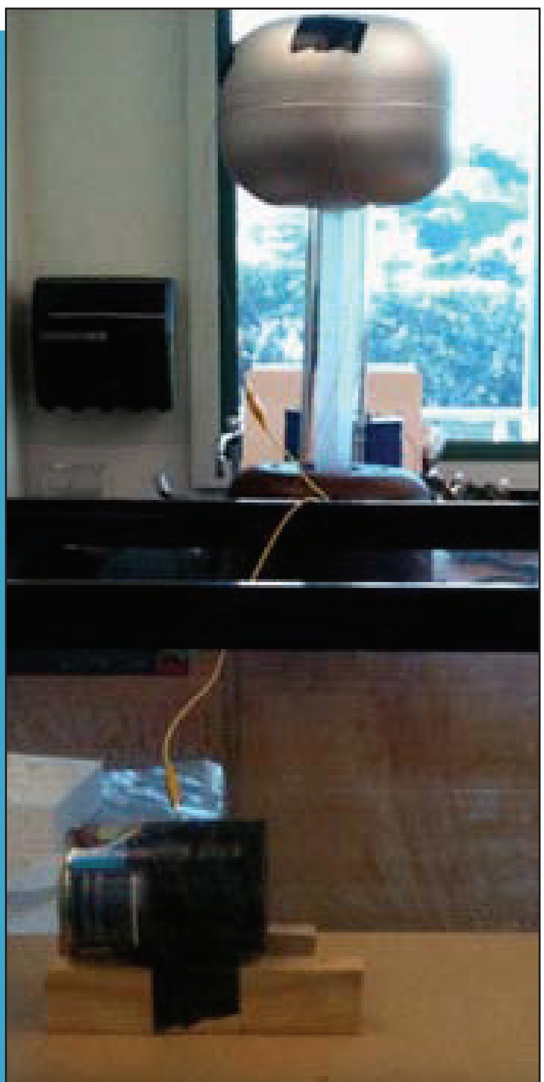

Introduction:

In our project, we will be testing the electromagnetic repulsion of the electrically charged smoke rings to the zinc plate. We already know that when rings collide, a specific pattern is created if the two rings collide at the same velocity. We based our project off of this experiment and wanted to add electricity to the experiment.

We will observe what happens when the smoke rings are shot at the zinc plate. If charged with enough electricity, we predict that the smoke itself will take on that charge, therefore repelling off of the zinc plate.

Method:

Using the common principles of repulsion, the same charges repel and opposite charges attract, we will use this principle to figure out what would occur when the forces of the Vander graph generator charge the chamber and therefore the smoke.

Once the smoke machine fills the electrically charged chamber, hopefully the smoke particles will take on a strong enough charge for repulsion. The smoke rings will be shot at a metal plate by pushing in one end of the chamber, which is covered with rubber.

The chamber will be filled with smoke by a thin rubber tube connecting the two. We will shoot the smoke rings first without the Vander graph generator attached and then with the Vander graph generator attached and compare the differences when the smoke rings collide with the plate.

Results:

We first ran control trials with the Van de Graaff generator turned off. We then ran the experiment with the generator on in order to observe the affects of electrically charging the smoke and the zinc plate.

When the generator was on we observed that the smoke rings showed an increase in repulsion from the plate when the rings got close to the zinc plate. The exterior of the smoke rings also showed an inward spin after they bounced off of the plate.

From these results, we will now try to improve our experiment by conducting another experiment using a more powerful generator to try and simulate a stronger repulsion.

Studying Cosmic Rays through a Cloud Chamber

Jonathan Hsu and Jesse Orrall

Abstract:

Cosmic rays are particles of energy that originate from outer space. We will study these particles through a self-constructed cloud chamber. Cosmic rays produce trails of condensation within the chamber, as they ionize the super-cooled alcohol solution when they pass through. We will try to answer the question of whether they produce extra condensation, in addition to ionizing the alcohol. Once the chamber is completed, we will videotape the cosmic ray trails to observe them more effectively. If time permits, we will also begin making a spring-loaded accelerator for a small BB pellet, which we hope will break the speed of sound. This will test our hypothesis of whether cosmic rays produce condensation through breaking the sound barrier.

Introduction:

Cosmic rays are important issues to understand when confronted with climate change, electronics, and space travel, just to name a few. Heavy exposure can result in cancer, DNA mutilation, and other effects commonly associated with radiation. Our objective is to understand the nature of cosmic rays through a cloud chamber and possibly discover why the particles ionize the alcohol solution. We hypothesize that the cosmic rays are traveling faster than the speed of sound, which would cause a trail of condensation, similar to an airplane breaking the sound barrier.

Formulation/procedure:

First, we must build the cloud chamber. The cloud chamber is a simple mechanism. It is made from a 6"x6"x12" airtight box made of acrylic glass with a piece of absorbent material at the top. There is a metal sheet and a piece of thin cardboard at the bottom of the container. The absorbent material at the top is soaked with isopropyl alcohol and dry ice is placed under the metal sheet. The dry ice super-cools the alcohol solution, which will in turn be ionized by cosmic rays.

Later on, depending on the time, we will see if a bb traveling faster than the speed of sound will produce the same type of condensation trail as a cosmic ray particle does. If the same result is observed, we can assume that the cosmic rays are in fact traveling faster than the speed of sound, and it is their speed that causes them to ionize the alcohol vapor. If not, we will continue the investigation with another experiment.

Unfortunately, the original plan of the cloud chamber failed, in part to a poorly built acrylic chamber. We created the box using sheets of acrylic glued together by epoxy and sealed with caulking. However, this chamber was not airtight and ended up falling apart. Therefore, we decided to take a different approach. Instead of building the cloud chamber, we used a 1-gallon glass jar with a metal lid; the metal lid of the jar replaced the metal plate under the box. We believed that using a jar with a screw on top would make our chamber airtight, and therefore, more successful.

[redacted]

"Cosmic rays are important issues to understand when confronted with climate change, electronics, and space travel, just to name a few."

Data/graphs:

In our first trial using the original box design, we used small dry ice nuggets in cylindrical shapes. We saw no cloud inside the box after waiting for several minutes. The holding tray was drenched in alcohol, and we noticed it dripping out of the container. We hypothesized that the container was not airtight and that the bottom of the container was not getting cold enough to super-cool the alcohol.

In our second trial, we attempted to fix those problems. We used duct tape around the base of the container to make it more airtight. We used thinner cardboard and a thinner sheet of metal for the container's bottom, so there would be a thinner barrier between

Jonathan Hsu examines the jar before conducting the experiment. (Left) The caulking at the bottom of the container that held up the sponge softened when it came into contact with the alcohol. The sponge fell, and we had to remake the container using a different adhesive.

Radioactive sample in cloud chamber produced no trails of condensation

the dry ice and the alcohol solution. We also used slabs of dry ice, instead of the cylindrical nuggets, hoping that slabs would have more surface area in contact with the metal sheet, and would therefore lower the temperature of the bottom of the container even more. However, we still saw no cloud inside the box after a long time. This time, the box was cold enough, but the duct tape around the container's bottom was still letting through alcohol. Again, the holding tray was drenched.

In our third trial, we used the jar for the first time. We used caulking to affix a thick car sponge to the bottom of the jar, which would hold the alcohol. The cloud was visible in the jar; however, it was very thin. We discovered that by turning over the jar, the cloud was much more visible, as if all the alcohol was resting at the bottom of the jar. At this point, the cloud was not dense enough to see cosmic rays. We installed a lamp projector instead of the normal lamp. This made the cloud much more visible; it was still secluded at the bottom. After an hour, we discovered that contrary to our belief, the jar was not airtight. When we turned it over to shake up the cloud, alcohol started leaking out of the bottom of the chamber. This explained why the mist became thinner over time. It is possible that the mist was leaking out of the chamber. It could also be that the sponge was not absorbent enough, and couldn't hold enough alcohol. It might be that the alcohol was being used up too quickly.

In our fourth trial, we duct-taped the bottom of the chamber so that it would be airtight. However, about ten minutes after we started, the sponge fell from the top of the jar because the alcohol weakened the caulking that the sponge was attached with. At the very least, there were no leaks.

In our fifth trial, we finally observed a thick cloud. We believed there were no leaks again, which had been a major factor in the failure of our first three trials. However, the cloud slowly became thinner and thinner over time, and the sponge started dripping. This reinforced our belief that the sponge was perhaps not absorbent enough, but we also felt that we had poured too much alcohol in the chamber. We also moved our experiment from the basement to the first floor, hoping that cosmic rays might be seen easier, but no cosmic rays were seen, because the cloud was too thin.

In our sixth trial, we placed less alcohol at first. There was still mist but it was a bit thin. After some time, we put more alcohol into the sponge, and observed a thicker cloud. We placed a radioactive Geiger counter test sample in the container, hoping to test our cloud, to see if particles passing through could be observed. If we observed trails of condensation, we would at least know that our cloud was thick enough. However, neither cosmic rays nor radioactive particles were seen in the mist.

"Once our results have been recorded and analyzed, and our hypothesis has been confirmed, we can further our research..."

Analysis:

We attempted two trials for the first part of our experiment, creating the cloud chamber. We built an acrylic box using plates of acrylic plastic and sealing it with caulking.

After our failed first trial, we believed there were three major problems.

In order to fix these problems, we changed these factors in our second trial. We used slabs of dry ice for maximum surface area, used a thinner piece of cardboard, and a fitted metal sheet for maximum air tightness. However, the result was still the same.

Though we had planned to also accelerate a BB faster than the speed of sound and observe it in the chamber, we ran into several problems in trying to assemble the chamber itself. In our next trial, we plan on using a shammy cloth (much more absorbent than the car sponge), hoping that it will hold more alcohol, and sustain the cloud for longer. Once we get the chamber up and running, we will investigate more how we could put it to good use

Conclusion:

As mentioned previously, construction of the cloud chamber is underway. This will allow us to study cosmic rays and test why they create trails of condensation. To put it simply, why does the cloud chamber work? Once our results have been recorded and analyzed, and our hypothesis has been confirmed or disproved, we can further our research and explore the other properties of cosmic rays.

1 The **dry ice nuggets** didn't provide enough surface area contact, so no **vapor was produced.**

2 The **cardboard** was too thick, thereby **insulating the box** and also keeping the **temperature** too high.

3 The metal sheet was **too big** for **the box**, thereby not making it **airtight**.

Developing a Remote Nano Drug Delivery Mechanism

Ian Cinnamon

Abstract:

We are developing a micro-scale valve for delivery of nano-milliliter quantities to the brain of a mouse or rat. Using Lab on a Chip technology, the valve is cast on a thin sheet of glass with PDMS epoxy plastic. The final product will be computer molded. Using two separate chambers, a balloon segment and a drug flow channel, precise quantities of any drug can be released into the brain of the mouse.

Introduction:

Currently, when live mice need to be observed under the influence of a certain drug, the mouse is held down and the drug is injected. However, the stress the mouse experiences from this trauma possibly affects the reaction of the mouse and therefore the results of the experiment. Because of this problem, scientists need a method that allows a drug to be delivered to the brain of a mouse with the mouse's knowledge.

Also, mice are put in isoflurane and injected with drugs as they sleep. This, however, poses a new set of problems – isoflurane can react with the injected drug and cause unwanted or even adverse reactions.

Therefore, we plan to develop a device that will be permanently fixed to the brain of a mouse and tethered to a logic system that controls the flow of the valve.

Formulation/Procedure:

Using Lab on a Chip technology, precise micrometer channels can be quickly and easily manufactured. We plan to create a complex two tiered system, with each tier containing a single channel. The lower channel is for the drug to flow from the reservoir into the brain. On top of that channel is a small square "balloon" channel that is inflated and pushes down on the drug flow channel. It is inflated by a logic unit which fills the balloon with fluid.

"We plan to develop a device that will be permanently fixed to the brain of a mouse and tethered to a logic system that controls the flow of the valve."

When the balloon channel inflates, the pressure pushes down on the lower drug flow channel, cutting off the path from the reservoir to the brain. When the logic unit releases pressure from the balloon, it deflates allowing fluid to flow from the reservoir to the brain once again.

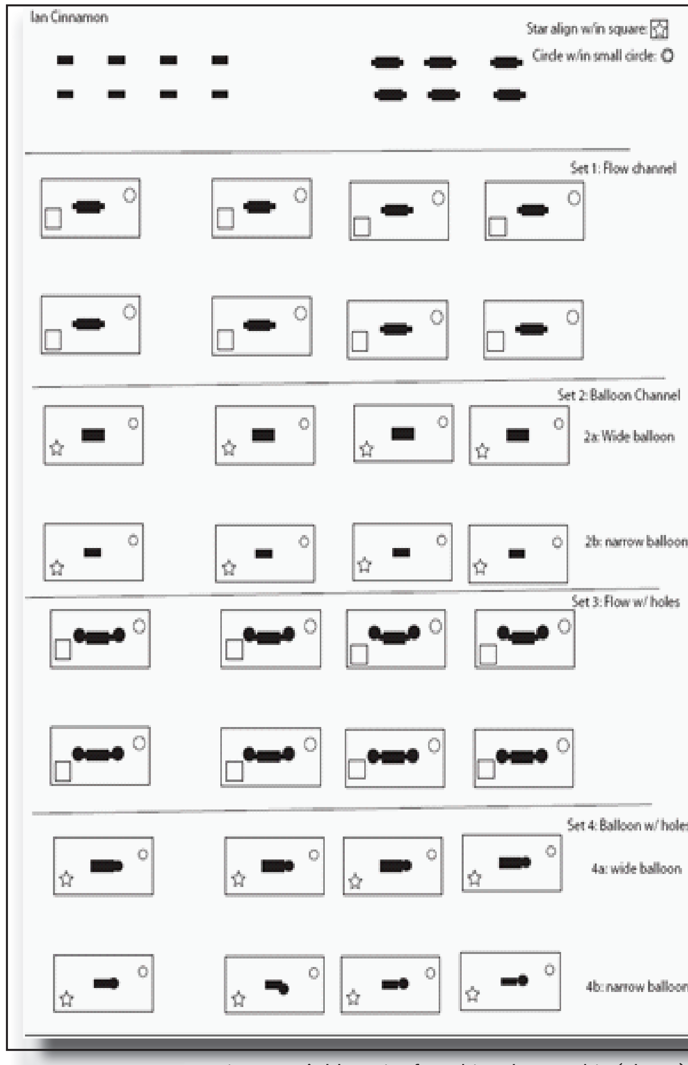

Ian Cinnamon's blueprint from his Lab on a Chip (above).

We have progressed through six iterations of the device, most of which can be seen on the informational YouTube video located at http://bit.ly/ianssr

Data/Graphs:

We have begun the manufacturing of the sample valves, and are using the same technique used in IC (integrated circuit) chip manufacturing. We created a negative of each layer of the mold which is then put on photoresist paper. The entire sheet is covered in about 0.2cm of PDMS plastic and then set to dry. Once it dries the PDMS is carefully cut out, removed and layered on top of the appropriate layers ,forming the complete valve. Like in IC prototyping, a single sheet of production valves contains dozens of trials with slightly different variations to speed up the process.

You can see the current device in action at:
http://bit.ly/ianssr

Hybrid Go-Karting

Riley Guerin and Niko Natsis

In the past, power and efficiency were inversely related. In order to gain power, efficiency had to be sacrificed; to become more efficient, power had to decrease. This can be seen in today's modern automobiles. The Toyota Prius can now average 50 MPG, yet has less than 100 HP. It can go over 500 miles on a single tank of fuel, yet takes about 10 seconds to reach highway speeds. The VW Jetta Diesel is another example. It gets nearly 50 MPG, yet is extremely weak and takes almost as long as the Prius to reach 60 MPH. The Tesla roadster can be seen on the opposite side of the spectrum. It is extremely powerful making nearly 250 HP from its AC electric motor. However, it can travel around 200 miles before being recharged. This makes it impossible for one to use it for a trip farther than a few daily errands and a visit to Marina del Ray from West Los Angeles. And lastly, the Bugatti Veyron is the prime example of power without efficiency. It makes an astonishing 1001 HP and can go 253 MPH. However, it achieves a pathetic 9 MPG average. This project is an effort to join power and efficiency. Neither will be sacrificed in our experiment and we are attempting to prove that the modern car industry can make both powerful and efficient gasoline, hybrid and electric cars.

Our cart is a String Ray steel chassis weighing in at nearly 183 pounds including motors. It has a roll cage which will eventually be fitted with solar panels to further increase efficiency. The motor will drive the rear left wheel and will be operated from the driver seat. While most car companies make hybrids where the electric motor and gasoline motor run independently of each other, our cart will be able to run both motors at the same time, as well as each one of them alone when either is needed.

At the moment, we are testing the gasoline motor extensively. We will determine the MPG while using 87 octane gasoline. Once this has been determined, we will test using a higher octane such as 89 or 91. After determining which octane fuel produces the highest average MPG, we will begin to use different mixtures of fuel. E85 as it is known is 85% ethanol and 15% gasoline. It is extremely powerful yet very inefficient. We will mix ethanol and gasoline to produce the best combination of power and efficiency. After this, we will test several more obscure forms of fuel such as methanol and vegetable oil. In the long run we are looking to include our electric motor as a substitute to running the gasoline motor at higher speeds. The electric motor does not have sufficient torque to get the kart going when friction is at its maximum at rest.

Our testing will take place only in the early morning during the coldest part of the day at a range of 50-60 degrees F. The kart will be rolled to the track and filled with between 250mL and 500mL of fuel. The weight of the kart will be an experimental variable and the direction it travels on the track will be as well. We will calculate the number of laps driven and use the amount of fuel consumed to determine the MPG.

Additional testing will be done on the effects of different climates and terrain. The kart will be driven on dry and wet concrete as well as on dry and wet grass. The kart will be tested turning only right and only left and it will be tested going uphill and downhill. This will allow us to determine how much the above listed factors contributed to the efficiency of the motor.

Our engine is a 163cc single cylinder gasoline motor. It is a 4 stroke motor that has its cylinder on a 25 percent inclination. The motor is air cooled and has a bore x stroke of 68mm x 45 mm. The cylinder is made from cast iron. It generates 5.5 horsepower at 3600 RPM and 10.8 Nm at 2500 RPM. To start the motor, a simple hand recoil system is used. The fuel tank can hold up to 3.6 liters of fuel and consumes 290 g/HP-hour. It holds .6 liters of oil and has a dry weight of 33 pounds.

Once our electric motor is added, we expect that our hybrid system will double the efficiency of the gasoline motor. Also, we will be using two different kinds of batteries in our experiment.

Most car companies use Lithium batteries, which are extremely efficient, yet not very powerful. One car company however, BMW, uses Nickel batteries, which are less efficient but much more powerful. We plan on setting up the battery cell in such a way that the lithium batteries will hold a large amount of electricity and give it to the nickel batteries after they have been used in short sprints when accelerating. This will again lead to greater power and greater efficiency.

Conclusion:

Our kart achieved an average 60.6 MPG. It was tested with both students in the kart. The Kart with both drivers weighs 503 pounds. The MPG was then tested again with each student driving alone. When the kart weighed 383 pounds, it achieved 69.7 MPG and when the kart weighed 313 pounds, it achieved 70.1 MPG. Therefore, when the weight of the kart is reduced by 40%, the MPG increased by 9.5 MPG or a fuel efficiency increase of 13.6%. We also varied the weight of the kart when testing braking. When the kart weighed 313 pounds, and accelerated for 15 feet, it then was able to stop in 46 feet. When the kart weighed 383 pounds and accelerated for 15 feet, it then was able to stop in 30 feet.

MPG Testing:

Date	Tanked filled with	Weight	MPG
Feb. 1-2, 2010	.5L	513 lbs	60.6
Feb. 4-8, 2010	.5L	313lbs	70.1
Feb 8, 2010	.5L	383lbs	69.7

Brake Testing—15′ acceleration:

Weight	Distance from full brake to full stop
313lbs	46′
200lbs	30′

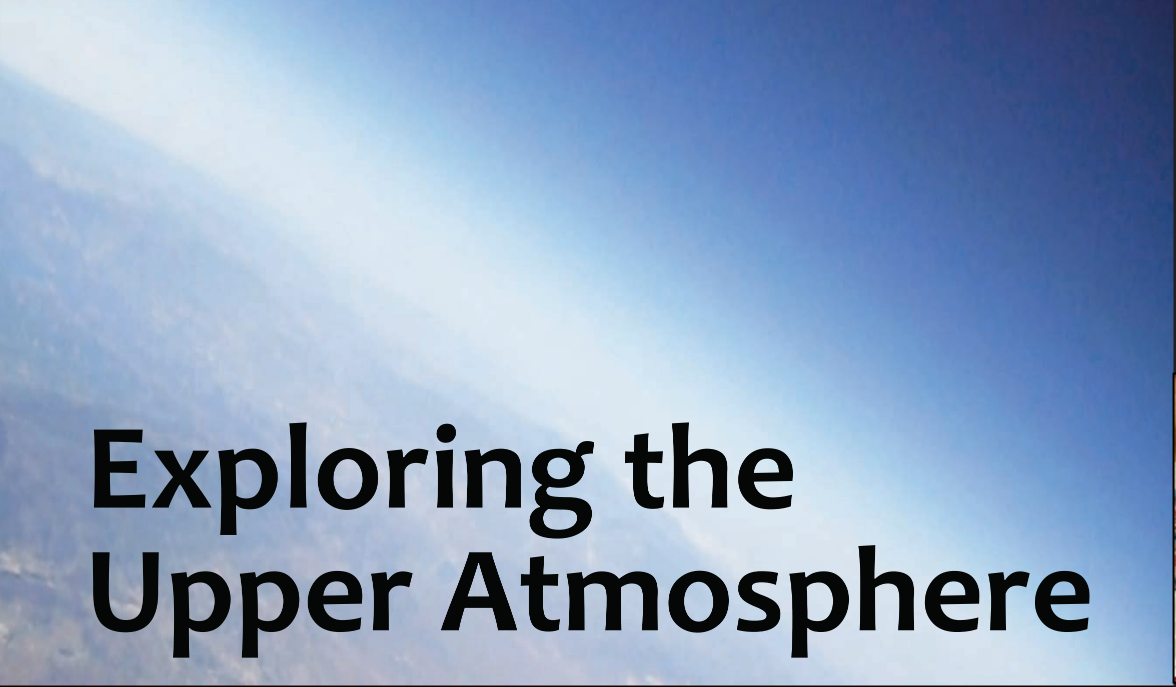

Exploring the Upper Atmosphere

Witten, Moelis, and Moody (from left) fix the wiring in their upper atmospherecraft.

Adam Moelis, Ryder Moody and Jacob Witten

We designed a craft that was taken high into the atmosphere (to 80,000 feet) by a weather balloon and recorded data. The craft took video from these heights so that we can see earth's curvature. In addition to taking video, later launches will ideally record measurements of altitude, temperature, and humidity. These flights will help us to understand the climate patterns of different levels of the atmosphere, as well as provide us the thrill of retrieving photographs we took from space. In order to ensure a successful flight, we had to research wind patterns at different layers of the atmosphere and plan our launch site accordingly. For recovery, we had a GPS-enabled cell phone.

Introduction

Taking images of the curvature of the Earth is worth it in itself, for their awe-inspiring nature alone. That said, it's not the only reason for Project Apollo. The first launch, to test the viability of the idea, only contained a camera. Due to its success, we can use more complex (and expensive) instruments to make more empirical observations, with important applications.

We hope to eventually send up instruments which record weather data, especially temperature, because of a key data point called lapse rate. Lapse rate is defined as -dT/dz, where T is temperature and z is altitude; in short, it is the rate at which the temperature decreases with respect to altitude. It has important ramifications on the mannor inffrared rays escape and cool the atmoshphere. Lapse rate affects the way the Earth cools itself, making it an important factor in determining some effects of global warming.

Procedure

First we created the shell of the craft, using a Styrofoam container. This provided the support and basic insulation for all of our components. Because the temperatures fell far below freezing, we also used heat packs to keep the electronics running. The insulated container had a small opening for the camera lens.

Once the container was built, we attached it to a weather balloon capable of lifting it. The balloon was designed to pop at our final altitude, so the craft then went into free fall. To prevent it from doing any damage a parachute deployed upon descent.

After the whole craft was built, we needed to attach electronics. The camera faced outward, taking video. A cheap GPS-enabled cell phone was purchased to transmit the craft's location in real-time to a computer so that we could track it. To actually find it, we installed flashers.

Test Run—March 14th, 2010

In preparation for the launch, we started up the heat packs, filled the balloon with helium and strapped everything into the box with duct tape. The positioning of the parachute presented a quandary, because we tried to put it in a position to deploy upon descent but we didn't want it to cause unpredictable air current effects during ascent. Eventually, we strapped it just under the balloon, assuming that the long fall would give it more than enough time to deploy. Finally, we got the cell phone's GPS software and the camera's time lapse photography started (at the last possible second, to preserve battery life), strapped the balloon to the box, and let go.

Actually, the first time we did this, we didn't fill the balloon with enough helium, but we quickly corrected that. The craft initially rose rapidly, but at an altitude of around 150-200 feet a gust of wind sent it downwards, where it hit a telephone pole and the balloon popped. Fortunately, at that point it was still visible, so we were able to recover the craft. Luckily, Everything but the balloon functioned perfectly. We successfully got GPS readings of the location during the (roughly 4 minute) flight, and we also got pictures—we even got a picture of a power line just as the balloon hit it.

Success – April 25th, 2010

We concluded from our test run that our systems were functioning sufficiently well to keep the same configuration for the next launch, with the small addition of an external charger for the cell phone so it wouldn't run out of battery. However, it was clear from our test launch we needed to increase the size of the balloon so we could use more helium and attain increased lift. We decided to use a balloon that was able to hold around 102 cubic feet of helium. We calculated that with a 2.4 lb payload, the craft would ascend at around 1100-1200 ft/min, bursting at its maximum altitude in only 80-90 minutes, perfect for maintaining battery life.

The morning of the launch, the Canon a470 we were planning to use malfunctioned, and we were forced to make adjustments last minute. We used a point and shoot video camera instead. Unfortunately, while we had modified the Canon to take extra lithium batteries, we did not have time to do the same to the video camera, so battery life ended up limiting what we got on video.

After launch, we simply had to wait for our GPS-enabled cell phone to transmit during its final stages of descent when it regained cell coverage at around 5,000 feet. This occurred approximately 2.5 hours after launch, when the craft was around 53 miles east of our launch site, which was just about what we expected. After searching through a square mile of brush because our last GPS reading was at about 1,000 feet, we finally were able to locate our craft and retrieved all its components completely intact. The impact of landing, we assume, pressed a button on the phone that exited its GPS tracking program, making retrieval quite difficult.

When we looked at the footage from the untested video camera, we found that the camera stopped working around 40,000 feet because the batteries ran out. However, up to that point, the camera worked perfectly, leading to breathtaking images like the one above.

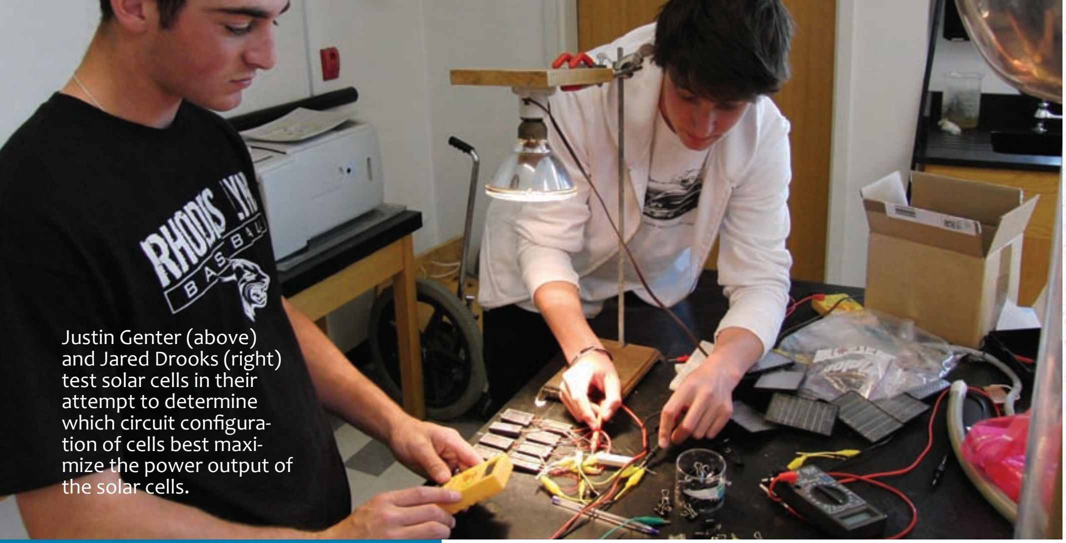

Justin Genter (above) and Jared Drooks (right) test solar cells in their attempt to determine which circuit configuration of cells best maximize the power output of the solar cells.

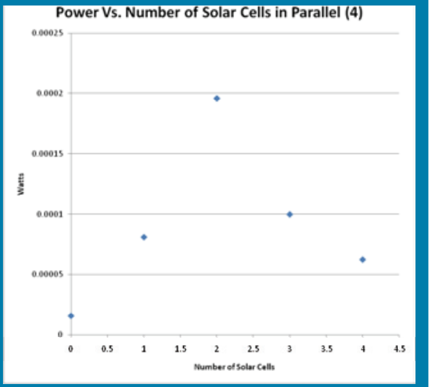

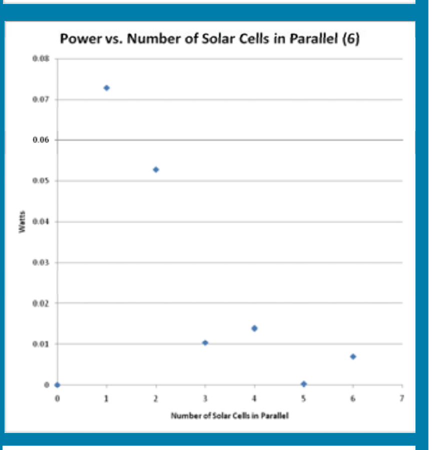

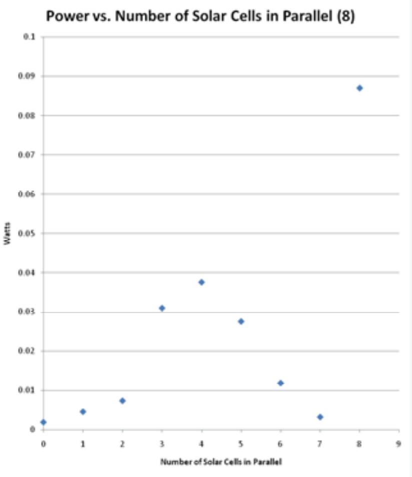

**For all the graphs (above), the numbers on the bottom represent the number of cells that are configured in parallel out of the total number of cells in the circuit. For example, at 1, one of the cells is configured in parallel, and the rest are in series.*

Maximizing Power Output of Solar Cells

Jared Drooks and Justin Genter

The purpose of our research is to find the most efficient way to arrange solar cells. Solar cells are already a clean and very useful source of energy and we are trying to find a way we can maximize the power output. Currently, companies that produc solar panels do not arrange them in the most efficient way. When the need more power, then just purchase another sheet of solar cells. If they researched optimal arrangements of wires for specific appliances, they would be able to generate more power from fewer solar cells. We set out to find the circuit configuration which maximizes the power output of the solar cells.

We obtained small solar cells and arranged them under a halogen bulb. The halogen bulb was plugged into the power socket and the light from the bulb created power in the solar cells. We used alligator clips to connect the cells together and kept the room lighting constant. In the circuits we used a 1 Ω resistor. There are two different ways that solar cells and can be arranged, in series, or in parallel. We first took data arranging four solar cells in all possible combinations of series and parallel. We then repeated this with six and eight solar cells. We then recorded the volts. Since we used a 1 Ω resistor it was very easy to discover the power. All we had to do to figure out the power was the square of the recorded voltage. Below are data tables of the power results that we recorded for each circuit pattern.

4 Solar Cells

Arrangement	4 parallel	4 series	3 series, 1 parallel	2 series, 2 parallel	3 parallel, 1 series
Power (Watts)	.0000625	.000016	.0001	.000196	.000081

6 Solar Cells

Arrangement	6 parallel	6 series	5 series, 1 parallel	4 series, 2 parallel	3 series, 3 parallel	4 parallel, 2 series	5 parallel, 1 series
Power (Watts)	.007	.0000423	.000313	.0139	.0104	.0529	.0729

8 Solar Cells

Arrangement	8 parallel	8 series	7 series, 1 parallel	6 series, 2 parallel	5 series, 3 parallel	4 series, 4 parallel	5 parallel, 3 series	6 parallel, 2 series	7 parallel, 1 series
Power (Watts)	.087	.00194	.00325	.0119	.0276	.0376	.031	.0074	.0046

After recording the data, we saw that our results were not consistent with each of the trials for the different number of solar cells. This proves our theory that there is not one specific pattern that is the correct configuration for all situations. At first we believed that arranging everything in all parallel would be the best way, but we soon saw from our test with six cells that this is not the case.

There is an optimum configuration for each specific situation to produce the most power, and testing for each situation is needed in order to figure out which way is best. If the companies who produce solar panels take into consideration what we have proven, than the number of solar cells needed to produce the same amount of power will be greatly decreased.

Geodesic domes, saving the world

Caroline Groth and Kristen London

One of society's most pressing problems is lack of housing for the homeless, and this problem is routinely exacerbated by natural disasters such as Hurricane Katrina and the recent earthquake in Haiti. After the earthquake, 1 million Haitians were left homeless and although half of these people found housing by March 2010, the conditions are still grossly inadequate. The rain and hurricane season, starting April 1, also leaves little time for improving these conditions. The current housing options, consisting of tents and other shelters made of bed sheets, sticks, and wood, will not protect against the looming torrential rains nor will they withstand Port au Prince's roads turned into giant rivers, a yearly event. These floods will worsen sanitation conditions even further as corpses and rubble are unearthed and taken through the city streets. Even prior to the rain though, the sanitation conditions within the current housing pose a threat. Without proper structures, food cannot be kept clean and sterile medical treatment cannot be provided; the increase in deaths due to minor injuries from infection is a direct result of the contaminated conditions. Ultimately, the current housing dilemma must be solved before the next natural disaster strikes, in order to ensure the safety of people all over the world. The optimum structure would be sturdier, have quick set-up time, be cost efficient, and also be able to withstand aftershocks or torrential storms. Geodesic domes are the perfect solution.

The Geodesic Dome, patented in 1954 by Bucky Fuller, is an extremely strong structure. Furthermore, its small surface area to volume ratio due to its spherical shape makes it very cost effective. The Dome consists of an icosahedron, built through a combination of triangles. The varying dimensions of the triangles allows the force to be spread evenly over in the structure, thus maximizing the strength. Also, the struts are relatively short so there is very little shear force, and the structure is less likely to snap in the middle of a piece of medal tubing. Lastly, because it is composed completely of triangles, the structure will not flex. The structure has the strength and space needed to provide housing for the Haitian homeless.

We decided to build a 2v geodesic dome, a simple dome that is relatively easy to build and it can go up quickly. The dome has a radius of 8 feet and is constructed of various length struts, 30 longer pieces and 35 shorter pieces. First we found desertdomes.com, a site that had a calculator that showed us what strut lengths we needed. We chose an 8' radius because the two different strut lengths can be easily cut from a 10' piece of metal conduit, eliminating waste of metal, and thus minimizing cost. We then cut the 30 long pieces and 35 short pieces from the 10' electrical metal conduit and flattened the

ends. The junctions were prepared by drilling 3/4' holes and inch and a half from either end. The dome was finally assembled using carriage bolts at the junctions. In order to seal the structure, we attached a tarp on inside of the metal cage at various points.

In the future, we plan to widely distribute these prefabricated structures. The various pieces can be prepared in America and sent in kits to various disaster sites to be built in about an hour.

Although the pieces are relatively small, we would like to look into an idea our classmate, Charlie Fogarty, had of a collapsible dome. The dome could be sent contracted and all you would have to do to build it would be to expand it.

Steam Power Renaissance

Will Hellwarth

Steam power is often considered an outdated mechanism of a past age, but in fact, steam powered is widely used in the generation of almost all of our electricity. High tech steam turbines that can withstand huge pressures and temperatures are used in lieu of the traditional steam pistons, and so they actually provide an efficient means of converting heat energy into motion energy like a traditional heat engine.

Steam power is often used as viable technology in speculative literary fiction, a genre commonly referred to as "Steampunk." While this often features fantastical contraptions, steam power is still a viable means of creating useful work for different motor driven utilities. Upon investigating current technology applied to the basic principles of steam power, converting energy in the form of compressed air or heat into mechanical work, the field has been left unexplored in favor of the exploitation of the gasoline internal combustion engine. However, stationary steam plants are still commonplace in the electrical industry. My thesis is that electrical generators that convert heat energy into mechanical work then into electrical energy, which is then used to generate heat and motion, are wasteful, not only in the energy conversion, but also in their fuel source and the efficiency of waste heat. By taking another look at steam technology, we can create a more eco friendly efficient solution to many everyday appliances.

The procedure will be to recreate a closed system steam engine, that instead of venting exhaust in the form of heat and decompressed water vapor, will cycle the waste products to maximize the energy generated from the coal burning and the buildup of water pressure, as well as the heat of the 'waste' steam as well. Most steam engines vent the waste steam because it is no longer pressurized, but already vaporized water is easier to recycle and re-pressurize than boiling water form a liquid, and it also contains a significant amount of heat energy, which we will absorb using similar techniques to the sterling-solar engine.

The idea of using steam power in place of electrical power is based off of the conservation of energy. Because there are fewer steps and conversions of energy from one type to another when using a steam engine for mechanical work than steam generated electricity, more energy is conserved. Because there will always be something lost in the conversion of energy, not to mention the resistance that siphons away electricity as it travels through miles of cable from a steam plant to the outlet, steam power straight to mechanical energy should be thermodynamically more efficient than electricity. Not only this, but a boiler can be heated by any means, which gives us flexibility over energy source. While coal would be the cheapest option, a steam engine gives us the option of an engine that can run off of almost any combustible substance, just so long as you can generate enough heat to boil water.

The Green Steam engine is an example of more modern materials brought to bear on a portal and efficient steam driven power source. About the same size as a conventional internal combustion engine of the same power, the green steam engine can be powered by any source that provides a pressurized gas, whether that be from a boiler, or any gas pressurizing machine. If it is powered by the boiler, the options for fuel sources can be anything that will burn or create heat. This allows for a very environmentally friendly engine that could be powered by solar cells, hydrogen cells, natural gas, or corn ethanol, among many other fuel sources. This provides a much cleaner solution than what is considered to be clean, electric motors, not only because an electric motor is charged by our power sockets fed mostly by dirty coal burning plants, but also because of the aforementioned loss of energy through the conversion processes.

Searching for
The Next Generation of Print Media

Sam Adams

Media technology is in a state of flux right now. Newspaper and other print media are falling out of business by the day and jobs in these fields are becoming increasingly scarce. It seems almost weekly when we see a new publication slashing jobs, closing up shop, or moving exclusively online.

This trend has been the prevailing source of concern for most people involved in the media industry ever since Google News became a major journalistic source. Everything appears to be moving online, but getting revenue from that is an incredibly dicey proposition; there is a monumental free-rider problem that hamstrings efforts of online news sources to support costly worldwide news reporting operations. Also, there is a sense of trustworthiness that comes with a tangible source—statistics have proven people are more likely to take earnestly data that someone took the time and money to publish. In an age of the often wildly-inaccurate "blogosphere," this credibility is a precious commodity.

But all is not lost. Though this transition is painful, the science is there to support a new wave of handheld media that can replace the newspaper without sacrificing journalistic credibility.

In the long run, it's probably a benefit that the print-based newspaper is on the way out. When you think about how wasteful the process of cutting down trees, converting them into pulp and then paper, using massive presses to imprint text and then a massive distribution network of trucks for delivery and then for recycling, the need for something new is obvious. We live in the digital age, and we should act like it.

We can see the forerunners of the next wave of "print" media consoles in stores today. The Amazon Kindle and Apple iPad are the kind of Internet-enabled reading devices that can display images with none of the production or distribution costs that make the newspaper industry so outdated and obsolete.

However, there's a reason you don't see every person reading the morning news on one of these devices. The Kindle only displays in black and white, and its design is clunky in a way that is reminiscent of first-generation iPods. Apple's product suffers from the backlight curse, which strains readers' eyes over a long period of reading.

There is in development a generation of "e-paper" that will alleviate these problems and take over the newspaper's throne as dominant print media. Using a complex optical procedure known as electrowetting, a small electric charge can create a black and white or color image.

In the reporting of this article, I tinkered with setups using this technology, which is essentially a glorified electric grid with specialized ink sprinkled upon it. If one laminates this with malleable plastic, one could create a flexible sheet of electronic paper that could fold like a newspaper, but be wirelessly updated daily with a new edition beamed directly from the newsroom..

Imagine, instead of having the New York Times delivered to your doorstep, you have it streamed to your broadsheet of e-paper. With optical technology that is in development, this is possible.

Researching on the edge

Last summer, more than a dozen students worked in labs across the country. Here's a selection of projects.

- ***Ian Cinnamon '10- UCLA***
  Bioengineering: Constructing a nano valve for implantation into the brain which can be controlled via cell phone.
- ***Yujin Park '10- UCLA***
  Biology: Working in a genetics lab to determine the function of every gene in a fly.
- ***Hanna Huang '11- Caltech***
  Biology: Studying the PHD12 gene in developing chick embryos
- ***Brian Hentschel '10- UCLA***
  Computer Science: Programming a sports scores iPhone app for UCLA.
- ***Kristen London '10- UCLA***
  Physics: Keeping track of data and results of various experiments.
- ***Katherine Casey '10- Michigan***
  Biology: Working with 25 other high school students on a variety of projects
- ***Spencer Horstman '10- UCLA***
  Computer Science: Studying human sound production via voice inflection.
- ***John Billingsley '10- UCLA***
  Astronomy: Determining brightness of objects in the IR spectrum from two different time periods
- ***Eva Levy '10- Cedars-Sinai***
  Biology: Working at the Gene Therapy Research Institute
- ***Caroline Sim '11- UCLA***
  Computer Science: Designing banners and website for green conferences.
- ***Claresta Joe-Wong '10- UCLA***
  Physics: Working with helium at a superfluidic state
- ***Brian Shultz '11- UCLA***
  Computer Science: Programming an iPhone app to aid in the lab's research
- ***Nick Duckwiler '11- UCLA***
  Biology: Collecting data on mouse experiments.
- ***Pauline Woo '10- Cedars***
  Immunology: Running gel electrolysis and PCR for other researchers
- ***Courtney Kelly '11- UCLA***
  Psychology: Processing data from lab's experiments

THIS ISSUE IS DEDICATED TO THE MEMORY OF BRENDAN KUTLER

Teardrop, 2009, photo by Brendan Kutler